# Lecture 5-8
# Instrumentation

## Requirements

### 1. Vacuum

- Mean Free Path
- Contamination
- Sticking probability

### UHV

- Materials
- Strength
- Stability
- Permeation

### Design considerations

- Pumping speed
- Virtual leaks
- Leaking
- de-greasing

## Vacuum pumps

- Diffusion
- Ion pumps
- Turbo molecular pumps
- Sublimation pumps
- Cryo pumps

## Sample handling

- Preparation
- Treatment in vacuum
- Manipulation

**Instrument : Light source, analyser, detector**

**Resolution, Sensitivity**

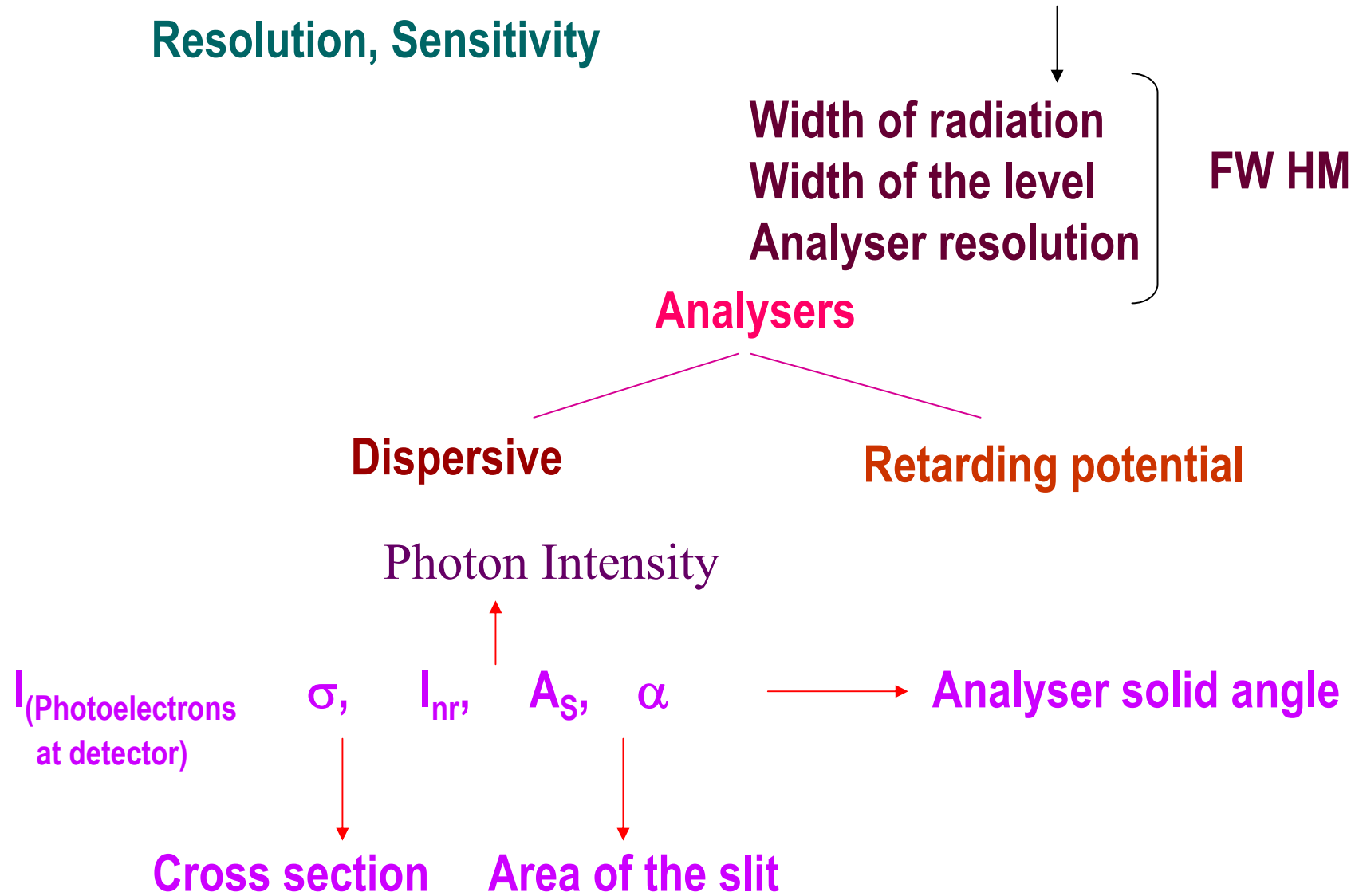

Transmission → Fraction of electrons reaching the detector from an isotropic point source

= Useful instrument solid angle . Transmission factor

Integral of point source transmission over slit area → luminosity

Integral of solid angle over slit area → étendue

Line width of radiation → pressure broadening
(Stark, van der Waals, resonance)

Doppler broadening
Recoil of atoms
Life time

$I(\theta) = 1 + \beta/2\,[3/2\,(\sin^2\theta) - 1]$ for unpolarised photons

$\beta$- asymmetry parameter

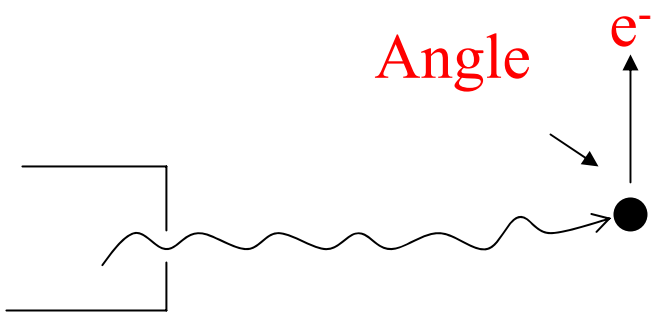


## Surface Sensitivity

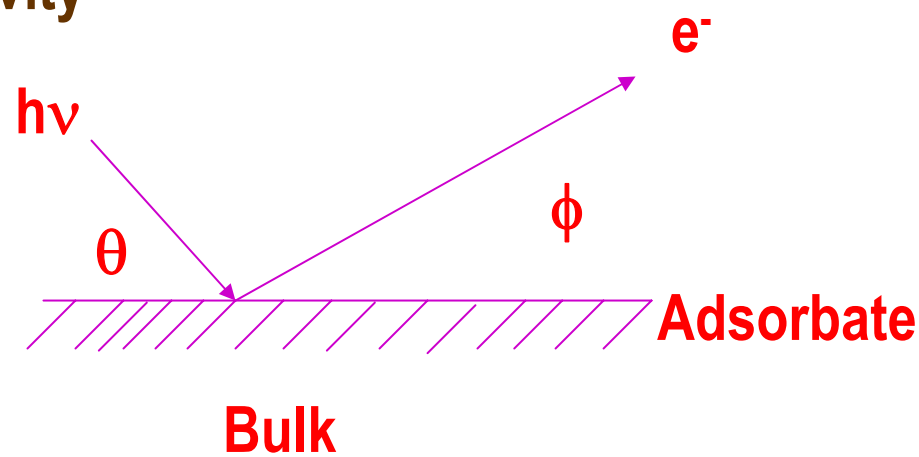

## Other techniques

Photo detachment
EXAFS, SEXAPS, synchrotron radiation

EPMA or Electron probe x-ray micro analysis

Ion beam techniques

SIMS
- dynamic
- static

ISS
RBS
FABMS

INS (ion neutralization spectroscopy)

SNMS (sputtered neutral mass spectrometry)
PIXE (particle induced x-ray emission

# History

Photoelectric effect 1887 Hertz

Rutherford β ray spectroscopy Before WWI

Basic XPS equation, $E_K = h\nu - E_B$ Originally stated by Rutherford 1914

Moseley After WWI

Rawlinson

Robinson β ray spectrum of elements

Anomalous lines corresponding to electron ejection due to fluorescence excitation.

Anger spectroscopy 1925

**Steinhardt 1951**

**"An x-ray photoelectron spectrometer for chemical analysis"**

**Kai Seigbahn – Uppsala 1940's**
**1967 "ESCA: Atomic, Molecular and solid state structure studied by means of Electron spectroscopy"**

**Acronym ESCA is due to Seigbahn**

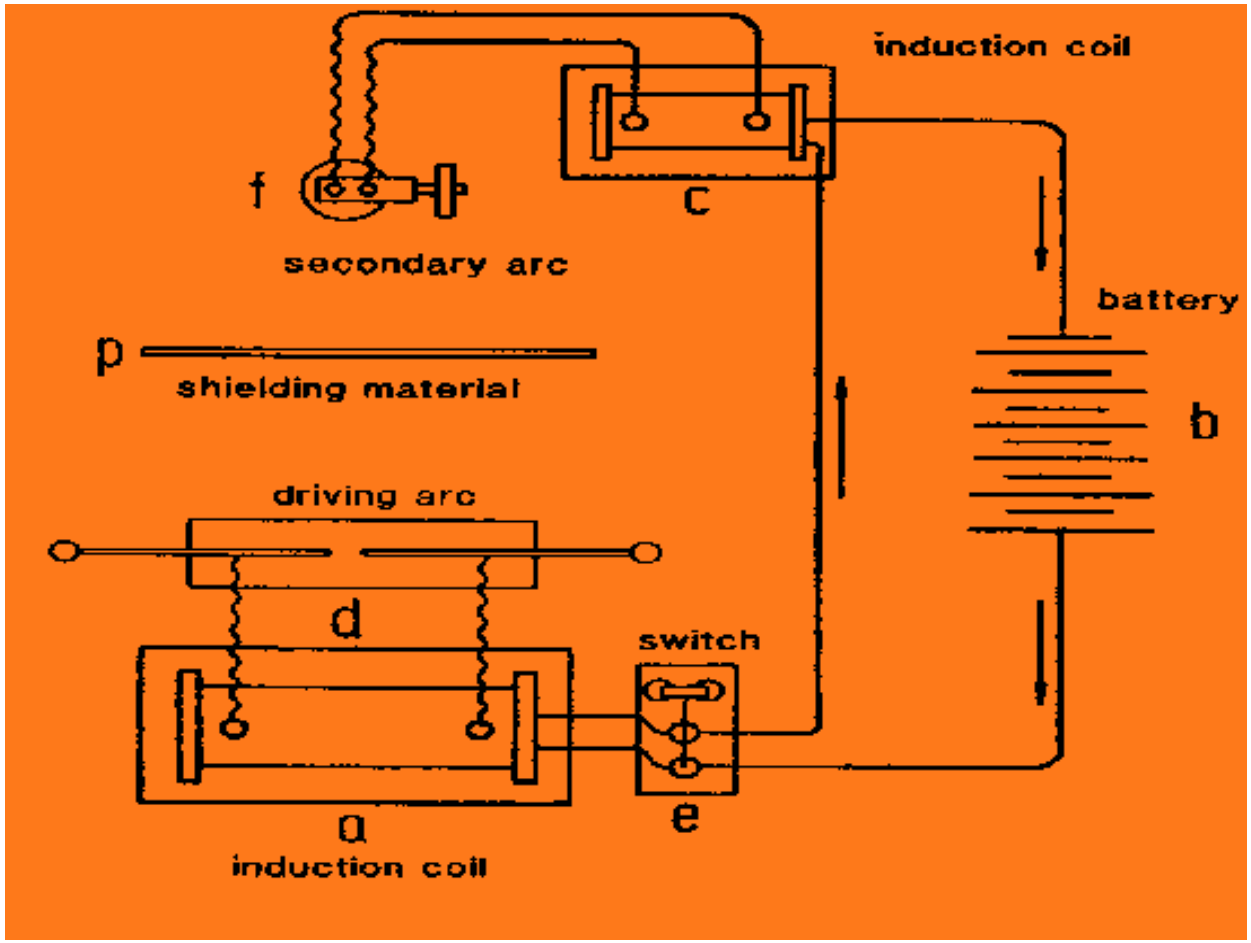


# Early Hertz Experiment

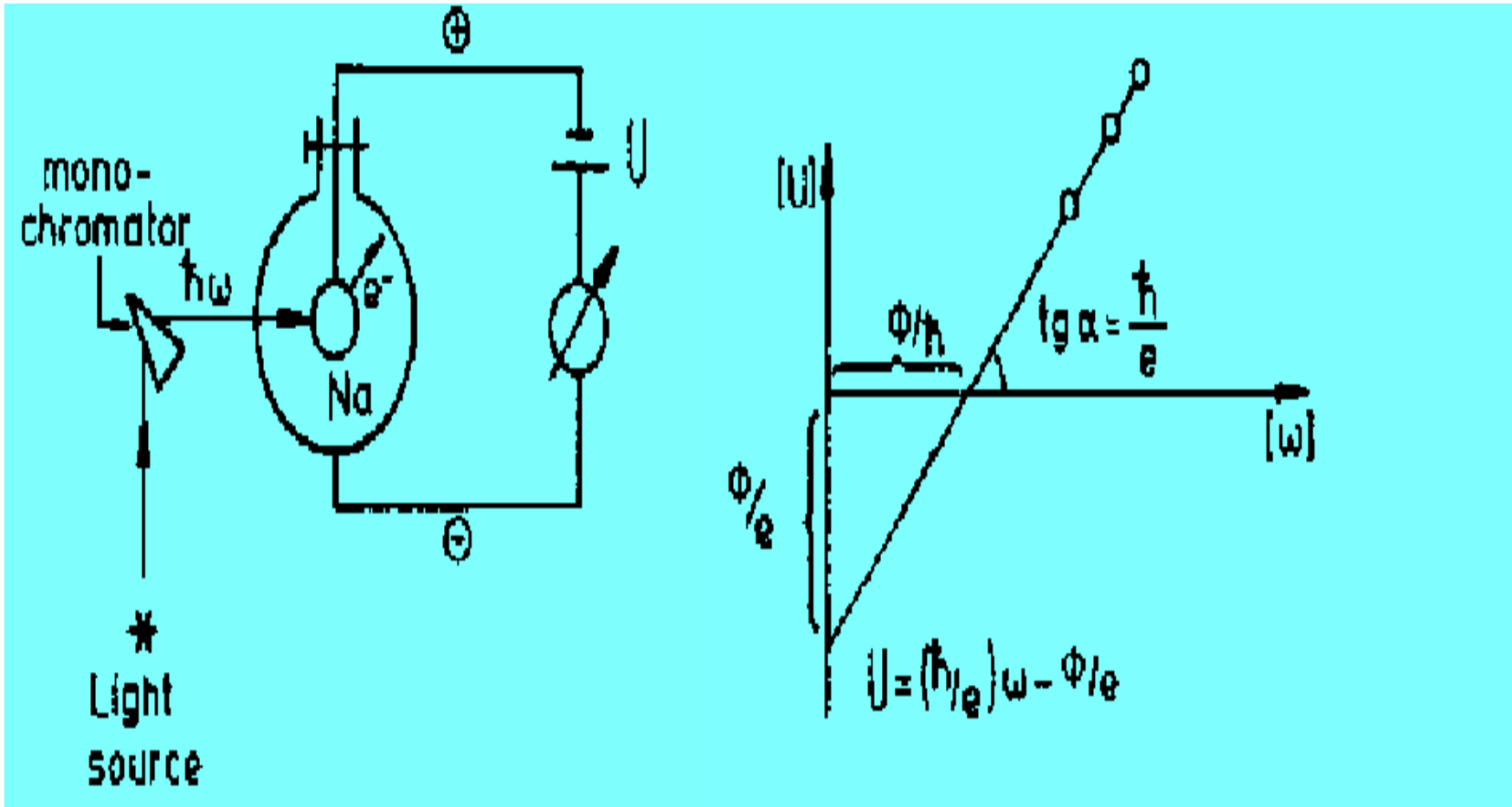
⊕
U
mono-
chromator
hω
e⁻
Na
⊖
Light
source
[U]
Φ/h
tg α = h/e
[ω]
Φ/e
U = (h/e)ω - Φ/e

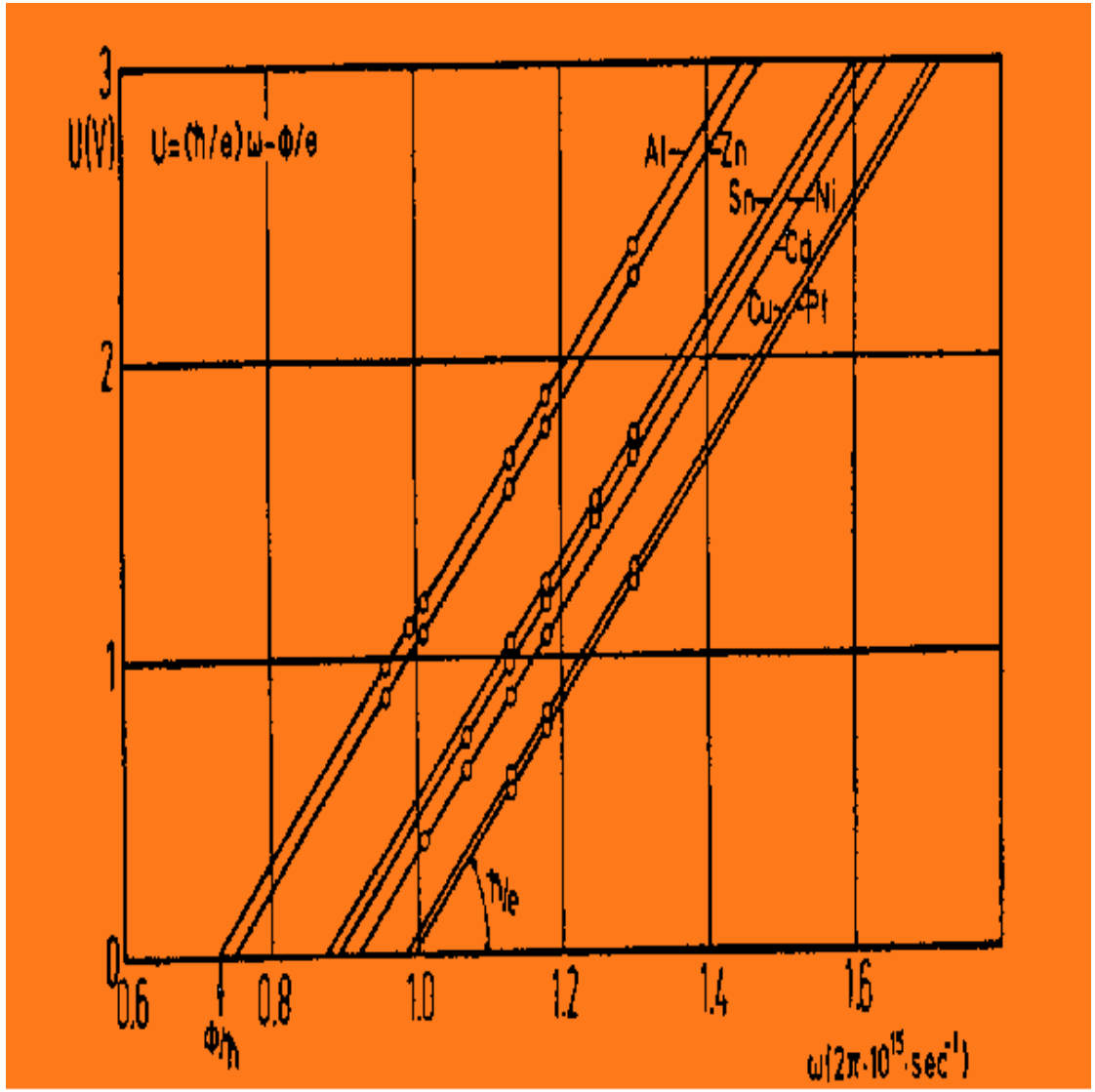


# U vs. ω for a number of metals

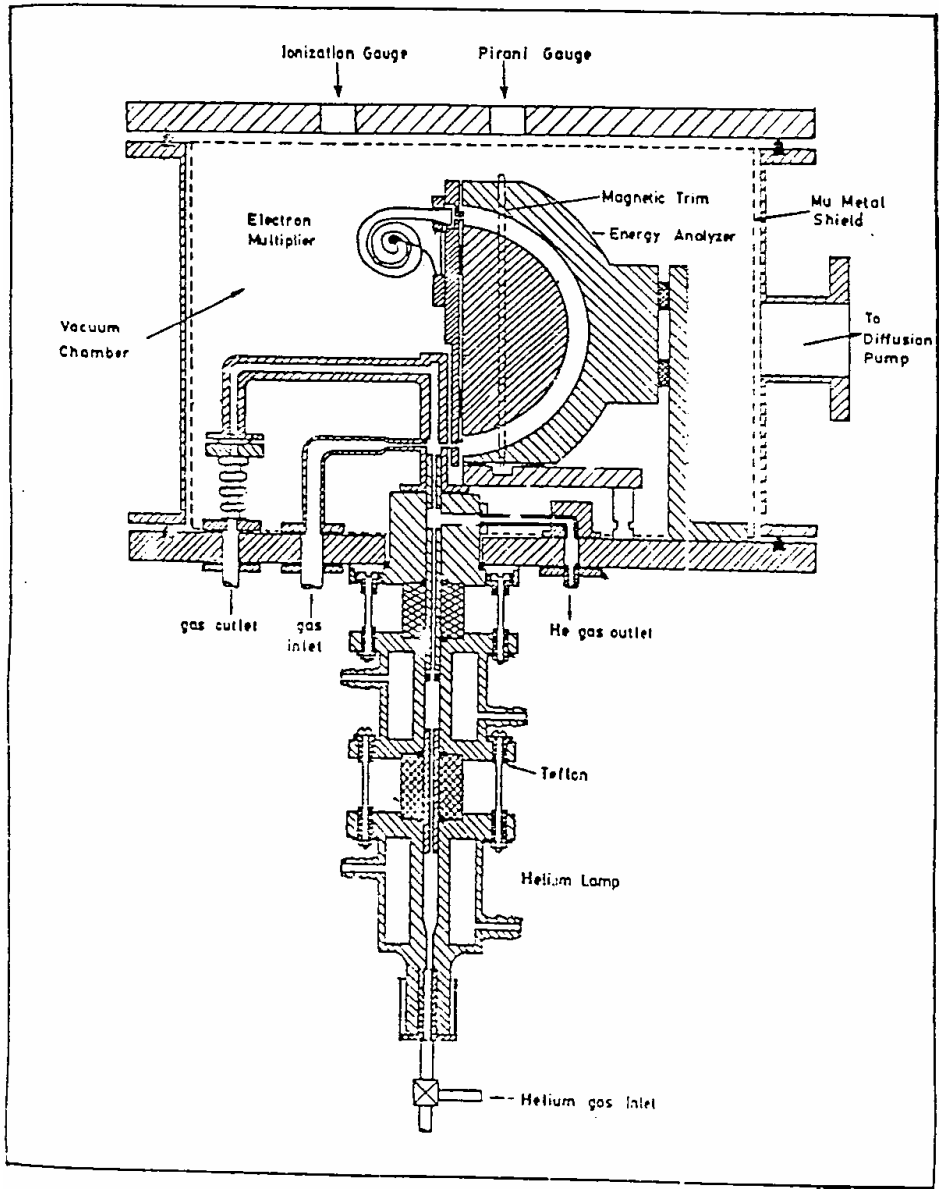
Ionization Gauge
Pirani Gauge
Magnetic Trim
Mu Metal Shield
Energy Analyzer
Electron Multiplier
Vacuum Chamber
To Diffusion Pump
gas outlet
gas inlet
He gas outlet
Teflon
Helium Lamp
Helium gas inlet

# Simple UPS

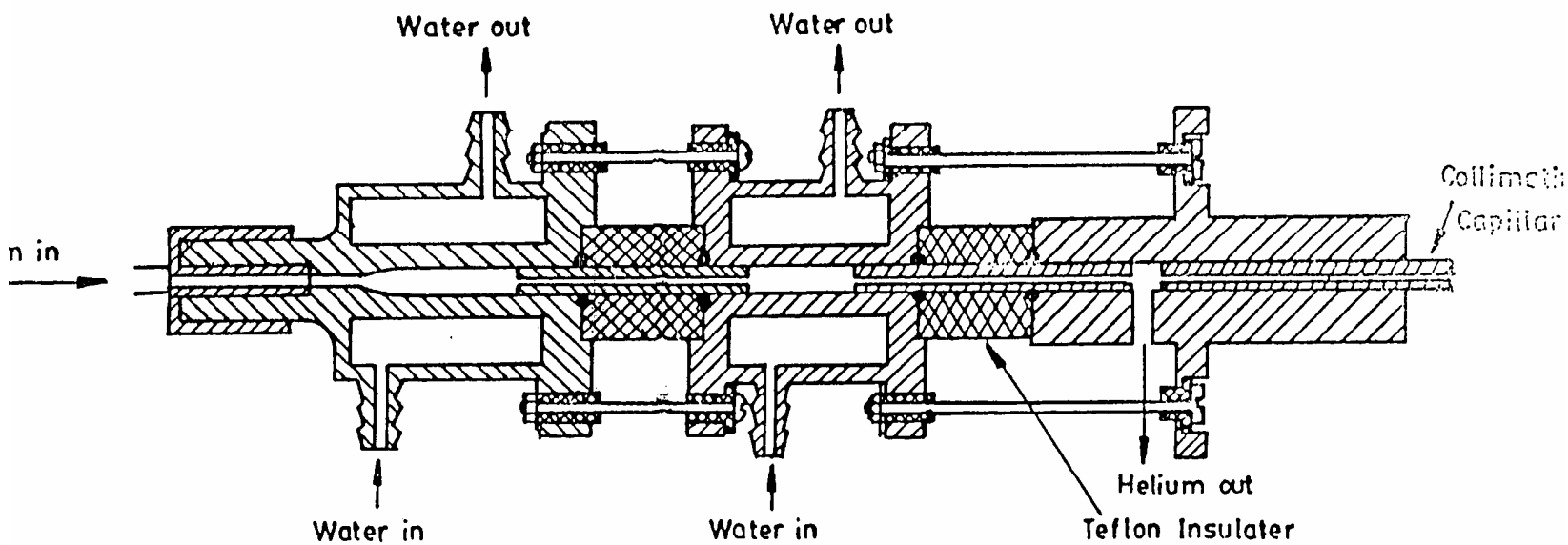


Fig. I.5. Cross-sectional view of the helium discharge lamp.

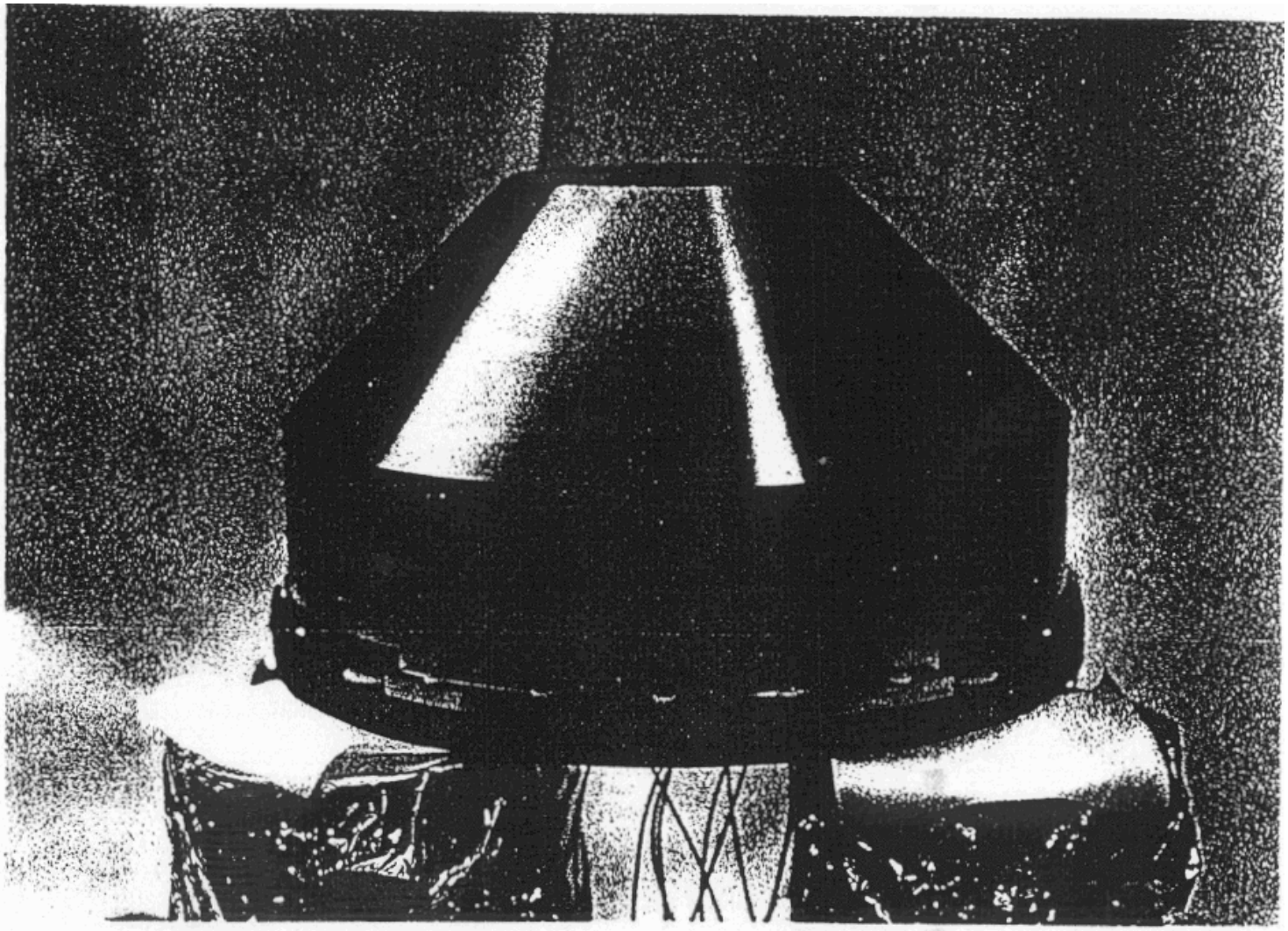

Heart of the instrument

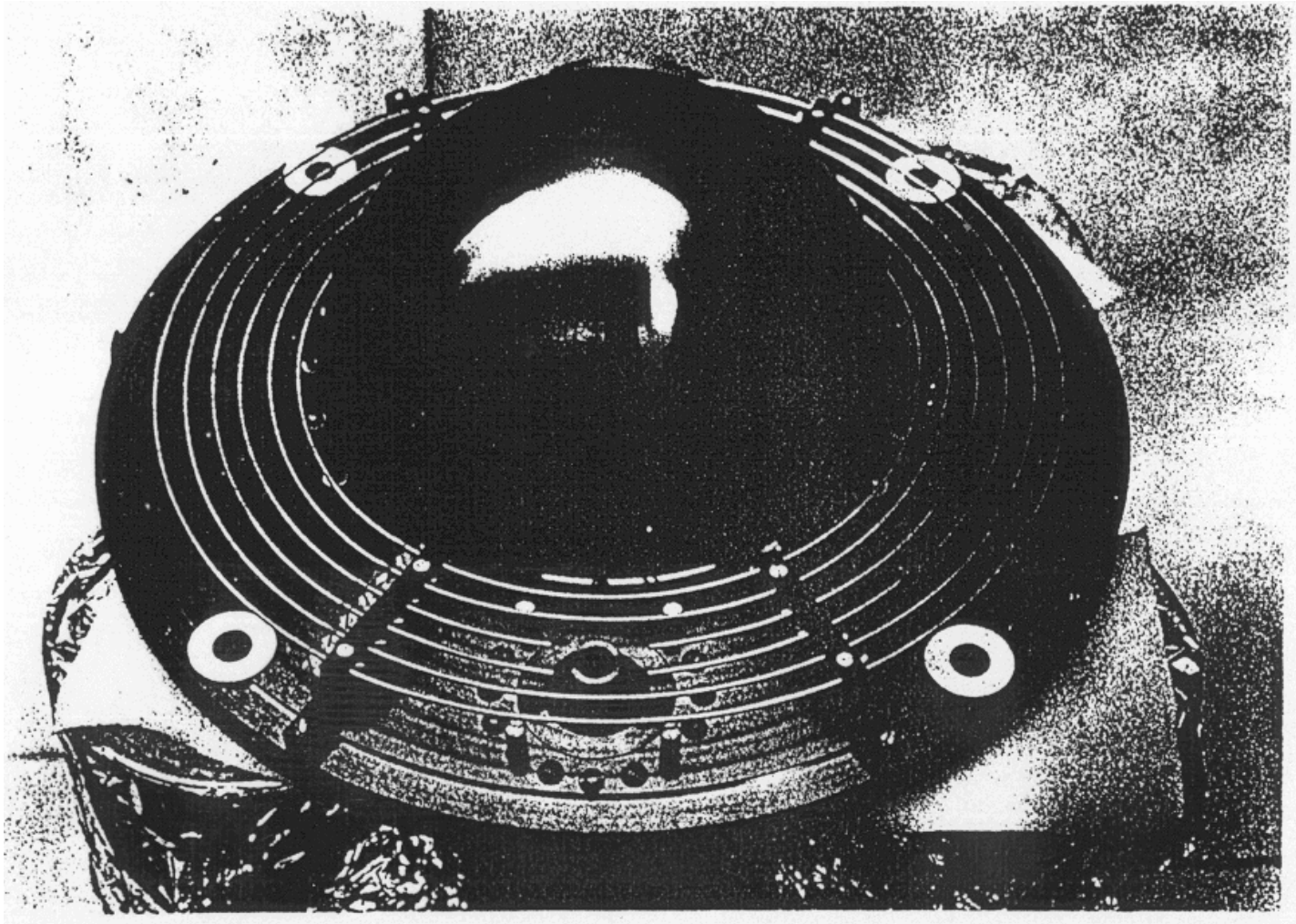

What is inside

# X-Ray Source

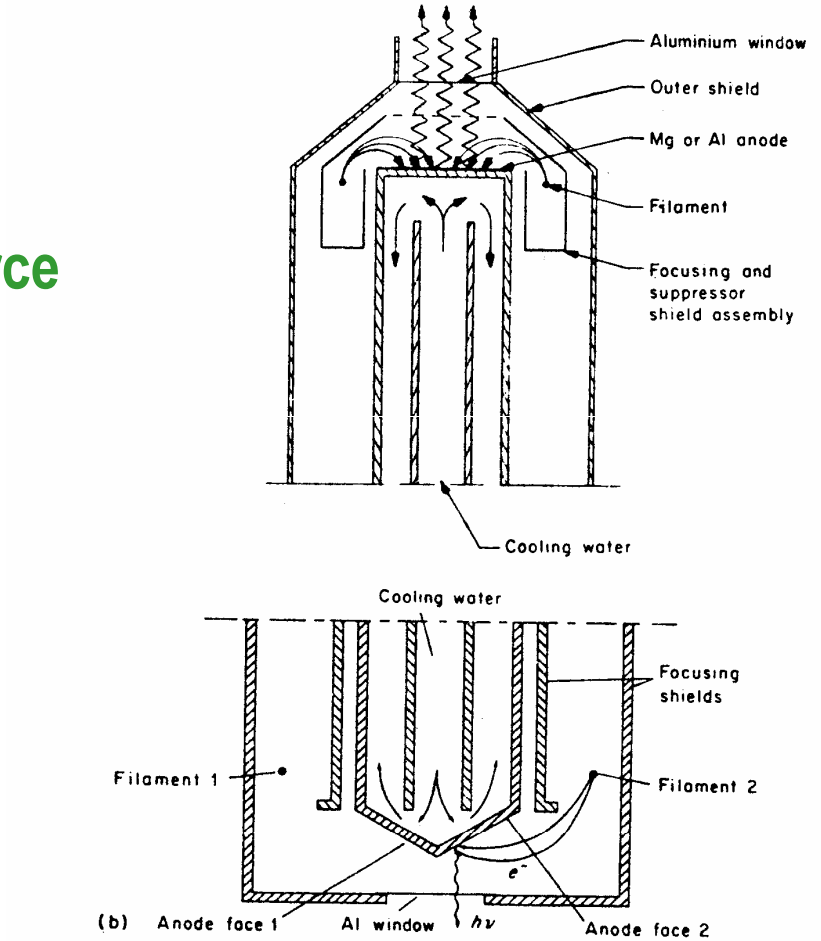


Figure 2.9 (a) Soft X-ray source with single anode of either magnesium
aluminium, deposited as a thick film on the flat end of a water-cooled copper bloc
The anode is surrounded by a cylindrical focusing shield at the same potential as th
filament. An outer can acts as a radiation shield and carries the thin aluminiu
window that must be interposed between the target and sample. (Reproduced b
permission of Perkin-Elmer, Physical Electronics Division) (b) Soft X-ray source wit
dual anode, allowing use of either magnesium or aluminium $K\alpha$ radiation by simp
external switching without the need to break the vacuum in going from one to th
other. The anode has a tapered end with two inclined faces on which films of ma
nesium and aluminium, respectively, are deposited. There are two semi-circular fil
ments, one for each face. The focusing arrangements are similar to those for the sing
anode of (a). (Reproduced from Barrie and Street[18] by permission of The Institute

# X-Ray emission spectrum

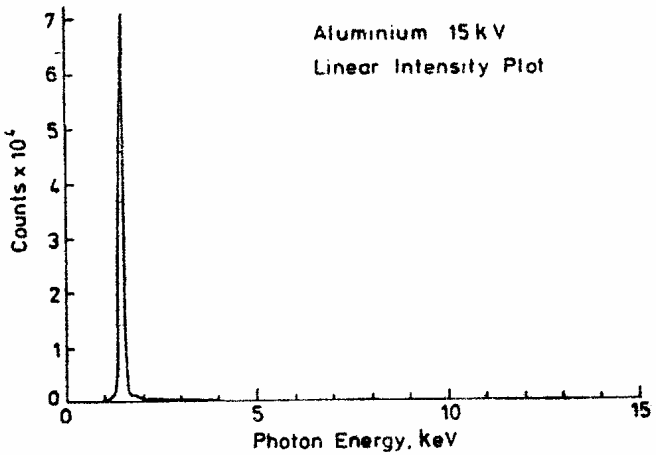


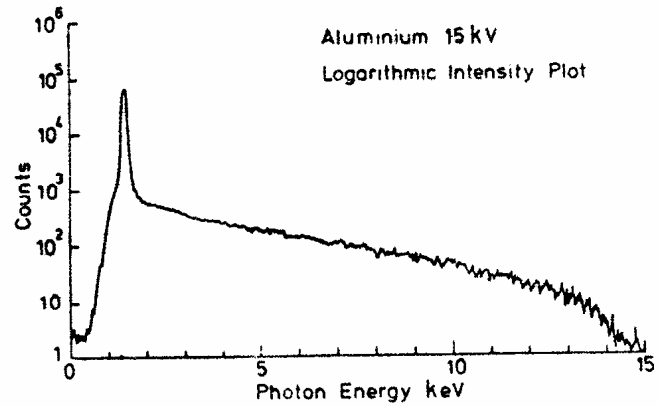


Figure 2.11 X-ray emission spectrum of an aluminium target under bombardment by 15 kV electrons, recorded by a lithium-drift detector through a beryllium window of thickness 7.5 $\mu$m. Upper curve, photon intensity plotted on a linear scale, on which little is evident except the intense characteristic $K\alpha$ line. Note that the energy broadening of the solid-state detector attenuates the peak by a factor of about 100. Lower curve, the same plotted on a logarithmic scale, that reveals more clearly the broad Bremsstrahlung background extending to energies much higher than the characteristic line. The background intensity at very low energies will have been reduced by absorption in the beryllium window. (Measurements by courtesy of Mr R. W. M. Hawes, Materials Development Division, Harwell)

# Detail of the spectrum

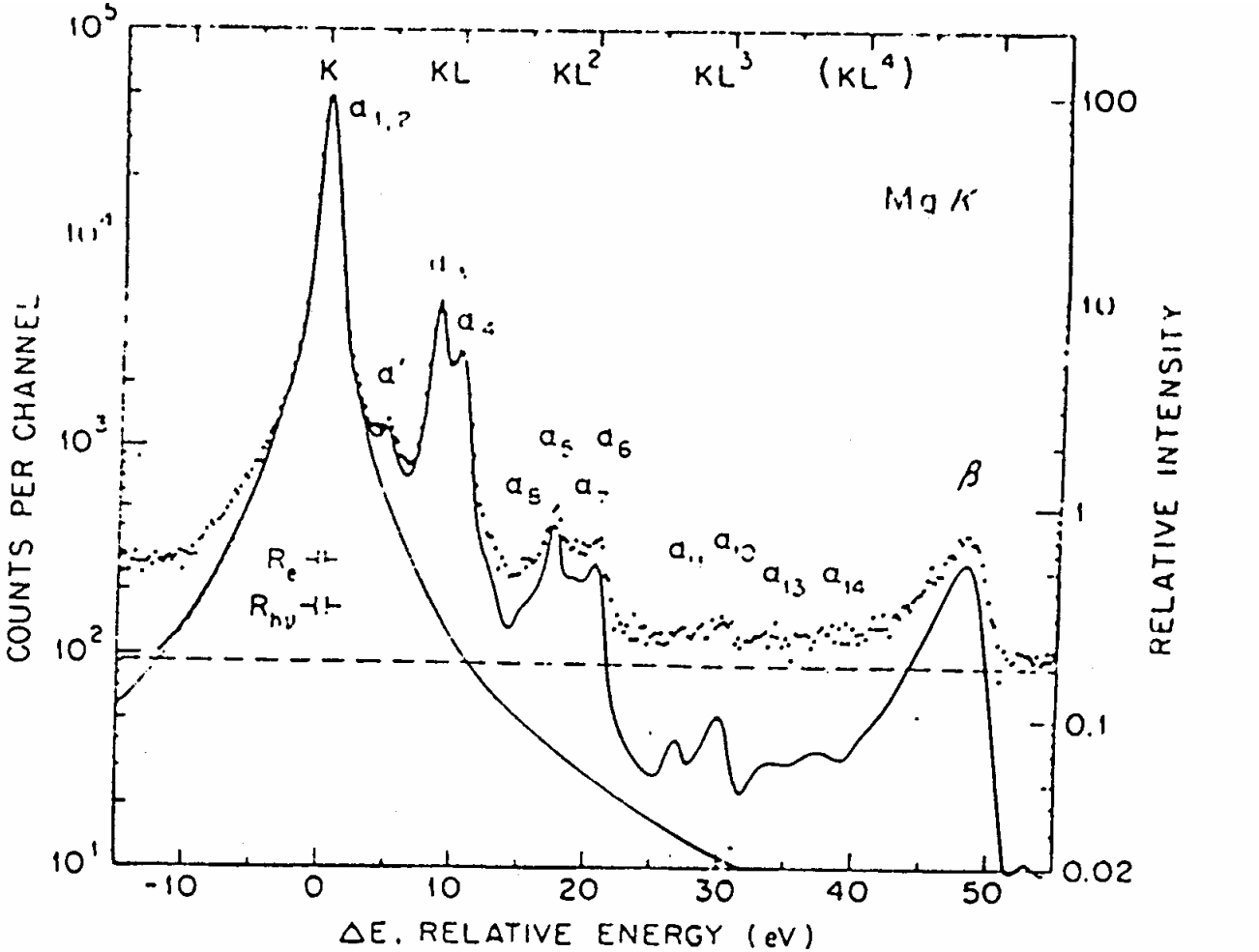


Fig. 2. The K x-ray emission spectrum of Mg metal as emitted by a non-monochromatized x-ray source. The peaks indicated $\alpha_1, \alpha_2, \ldots, \beta$ correspond to various transitions into the K = 1*s* subshell. The dashed line is an average background and the solid line is the net spectrum. Note the logarithmic intensity scale. The notation K corresponds to a single initial 1*s* hole, KL to initial holes in both 1*s* and 2*s* or 2*p*, $KL^2$ to a single initial hole in 1*s* and two initial holes in 2*s*, 2*p*, etc. (From Krause and Ferreira, ref. 37.)

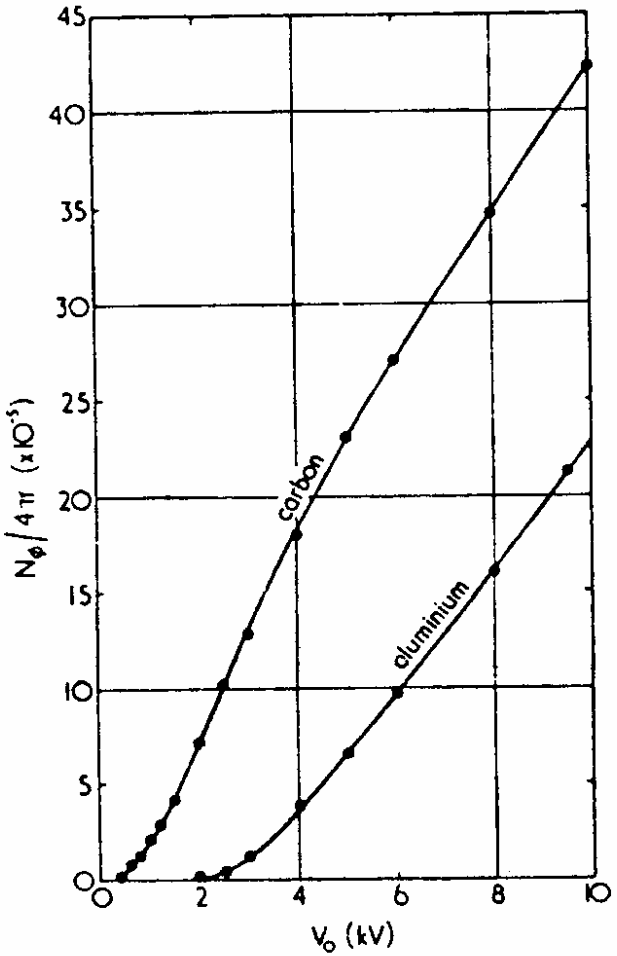


Figure 2.10 Dependence of efficiency of production of Al $K\alpha$ and C $K\alpha$ characteristic radiation on the energy of the bombarding electrons. (Reproduced from Dolby[20] by permission of The Institute of Physics)

Table 2.1 Energies and widths of some characteristic soft X-ray lines

| Line | Energy, eV | Width, eV |
|---|---|---|
| Y $M\zeta$ | 132.3 | 0.47 |
| Zr $M\zeta$ | 151.4 | 0.77 |
| Nb $M\zeta$ | 171.4 | 1.21 |
| Mo $M\zeta$ | 192.3 | 1.53 |
| Ti $L\alpha$ | 395.3 | 3.0 |
| Cr $L\alpha$ | 572.8 | 3.0 |
| Ni $L\alpha$ | 851.5 | 2.5 |
| Cu $L\alpha$ | 929.7 | 3.8 |
| Mg $K\alpha$ | 1253.6 | 0.7 |
| Al $K\alpha$ | 1486.6 | 0.85 |
| Si $K\alpha$ | 1739.5 | 1.0 |
| Y $L\alpha$ | 1922.6 | 1.5 |
| Zr $L\alpha$ | 2042.4 | 1.7 |
| Ti $K\alpha$ | 4510.0 | 2.0 |
| Cr $K\alpha$ | 5417.0 | 2.1 |
| Cu $K\alpha$ | 8048.0 | 2.6 |

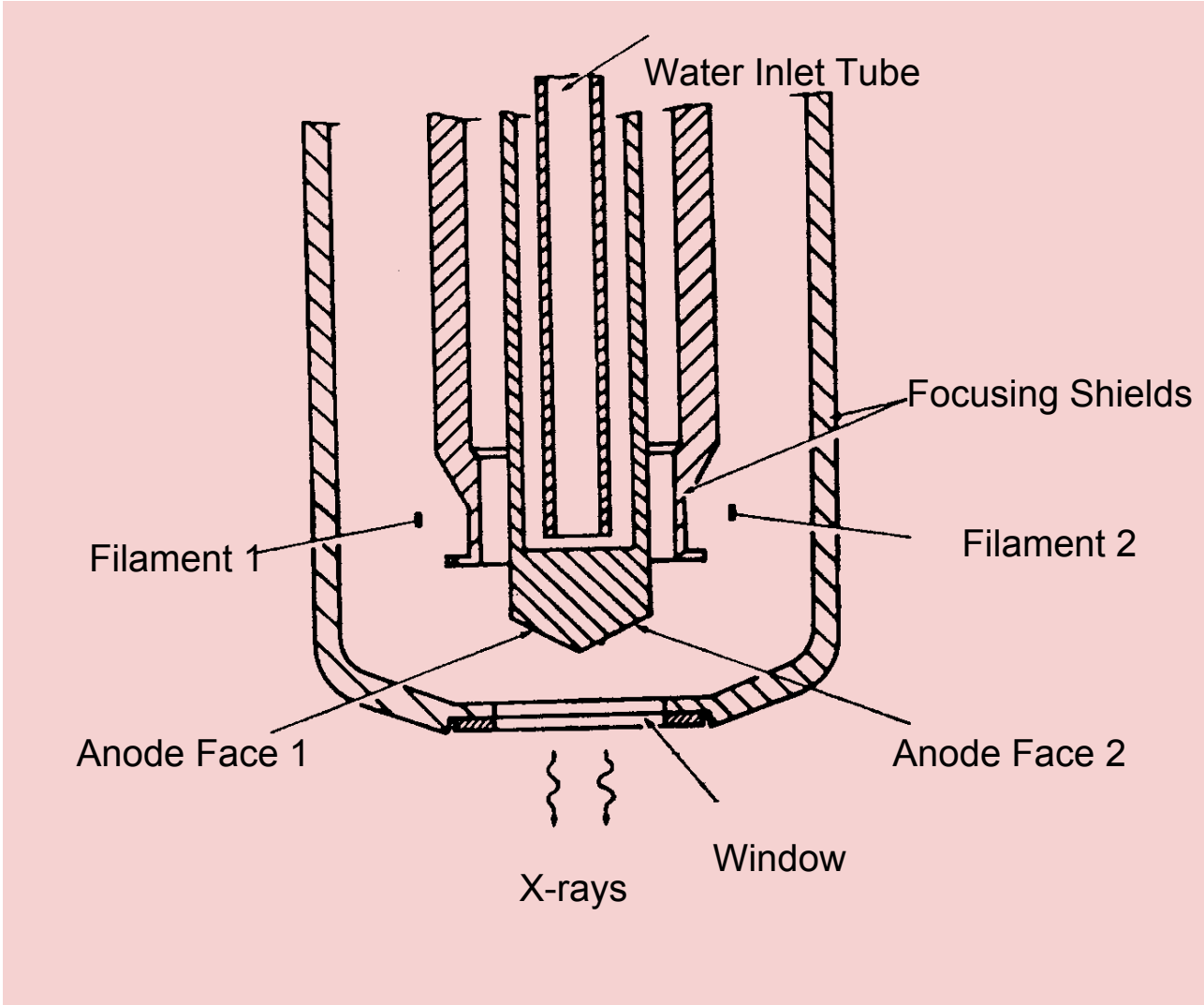


# X-ray source with dual filament and anode faces

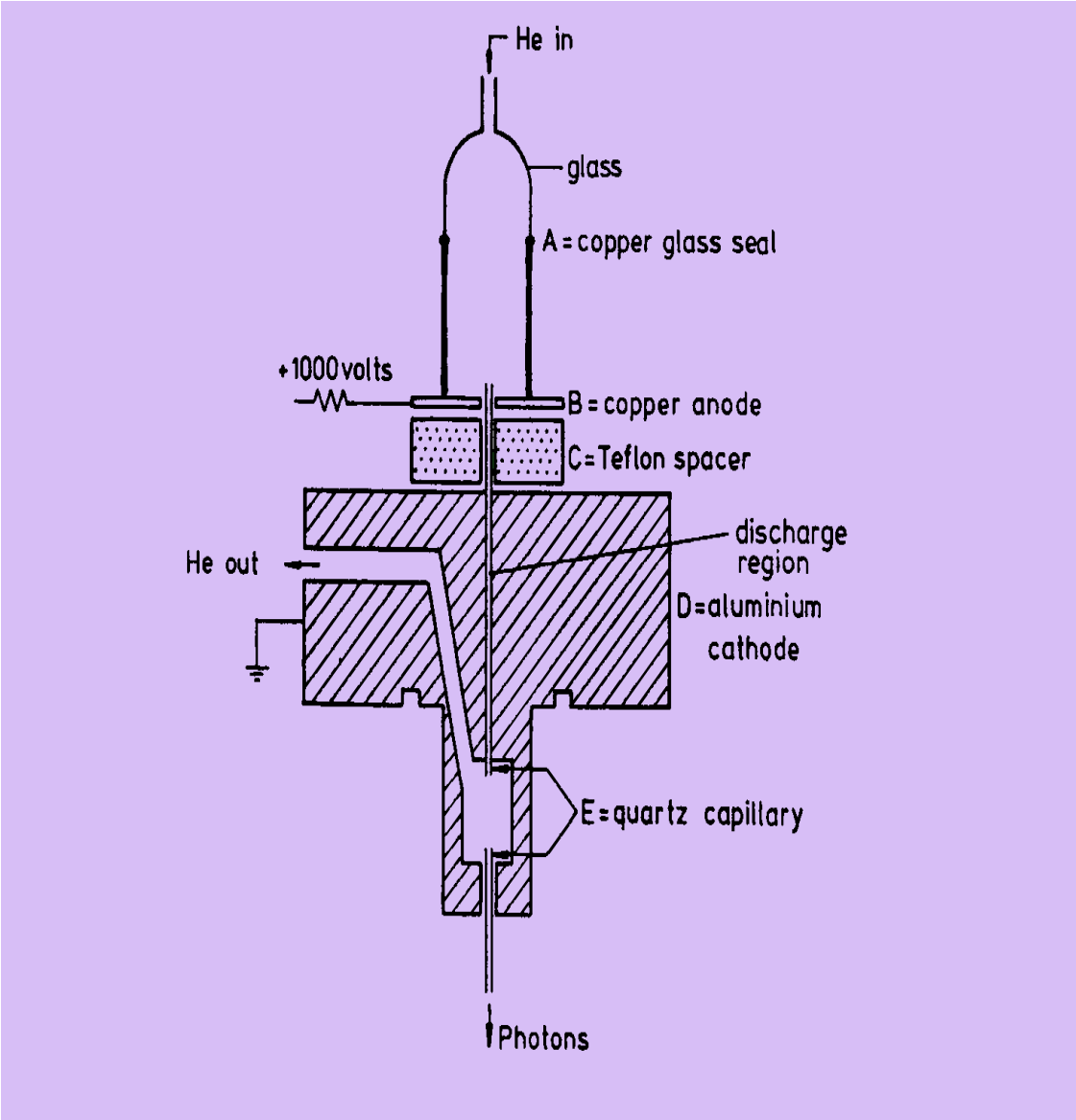
He in
glass
A = copper glass seal
+1000 volts
B = copper anode
C = Teflon spacer
discharge region
He out
D = aluminium cathode
E = quartz capillary
Photons

# UV Source

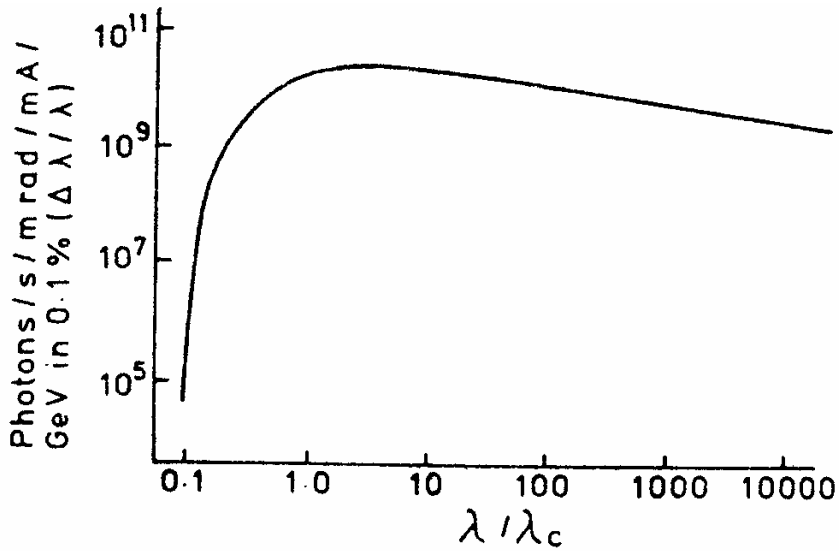


Figure 2.13 Shape of the radiation spectrum of an electron travelling in a curvec orbit. The vertical scale of photon flux is a function only of the electron energy anc current, while the horizontal scale is defined by $\lambda_c$, the so-called critical wavelength. I the maximum intensity is required to be at an energy near 1000 eV, then $\lambda_c$ should be 1 °A or less. To achieve that the orbiting electrons must be accelerated to severa gigaelectronvolts, and the radius of the orbit should be of the order of a few metres (After Farge and Duke[24])

# Synchrotron

# Resolution

Absolute resolution, FWHM $\Delta E$

Base width $\Delta E_B = 2\,\Delta E$

Relative resolution $R = \Delta E/E_0$

Represented normally, in percentage, $\Delta E/E_0 \times 100$

Resolving power $\rho = 1/R = E_0/\Delta E$

XPS line widths 0.7eV Mg $K_\alpha$, 0.85 eV Al $K_\alpha$, For an absolute resolution of 0.2 eV, the relative resolution is $10^{-4}$ or a resolving power of 10,000.

To keep the analyser size to an optimum value, the KEs have to be retarded - pass energy.

For an absolute resolution of 0.2 eV, the relative resolution is only $10^{-3}$. High absolute resolution can be achieved by retardation.

Not always advantageous.

Requirement in UPS

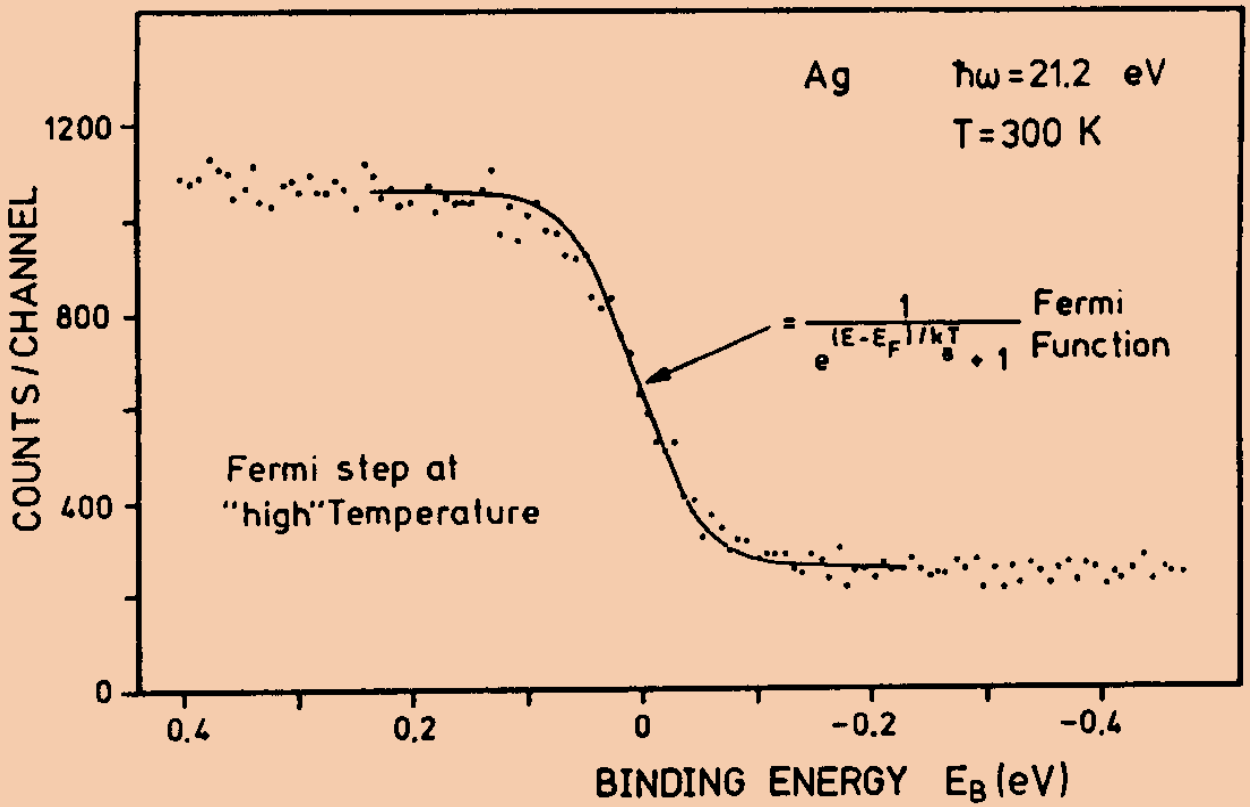


EDC around $E_F$ in an UPS spectrum of Ag. Solid line is the Fermi function at RT

# Electronic structure of solids

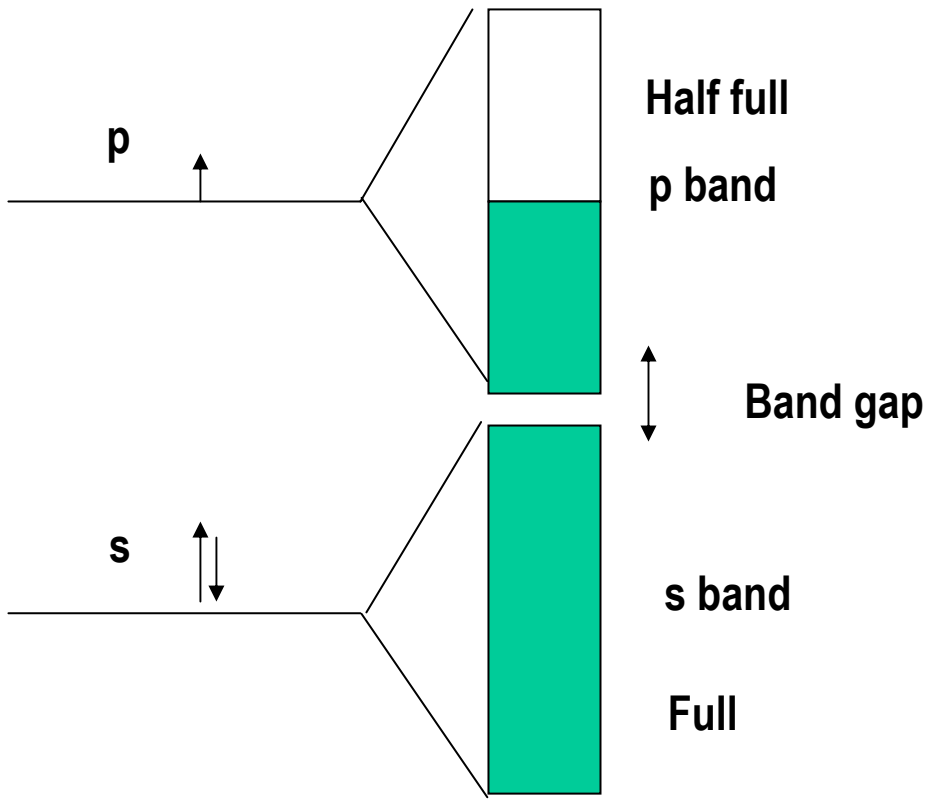

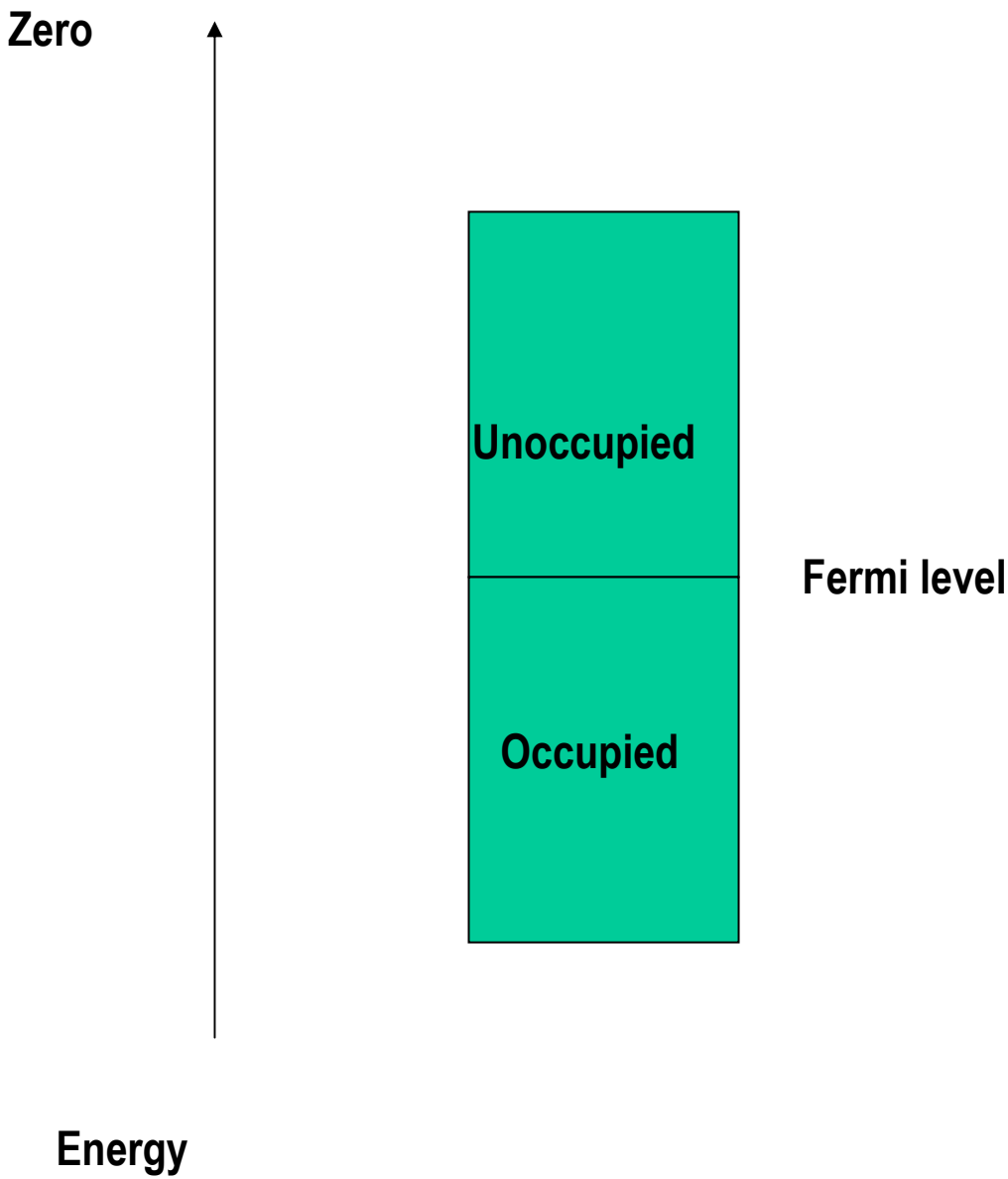
Zero
Unoccupied
Fermi level
Occupied
Energy

In a piece of metal, there are $10^{23}$ electrons.
We have high quantum states for most electrons.

Probability that a given quantum state is occupied is given by the **Fermi factor,**

$$f(E) = 1/[e^{(E-\mu)/kT} + 1]$$

Plot of this is given here which gives a definition of Femi level.

**μ is chemical potential, is the energy of the level for which f(E) = ½**

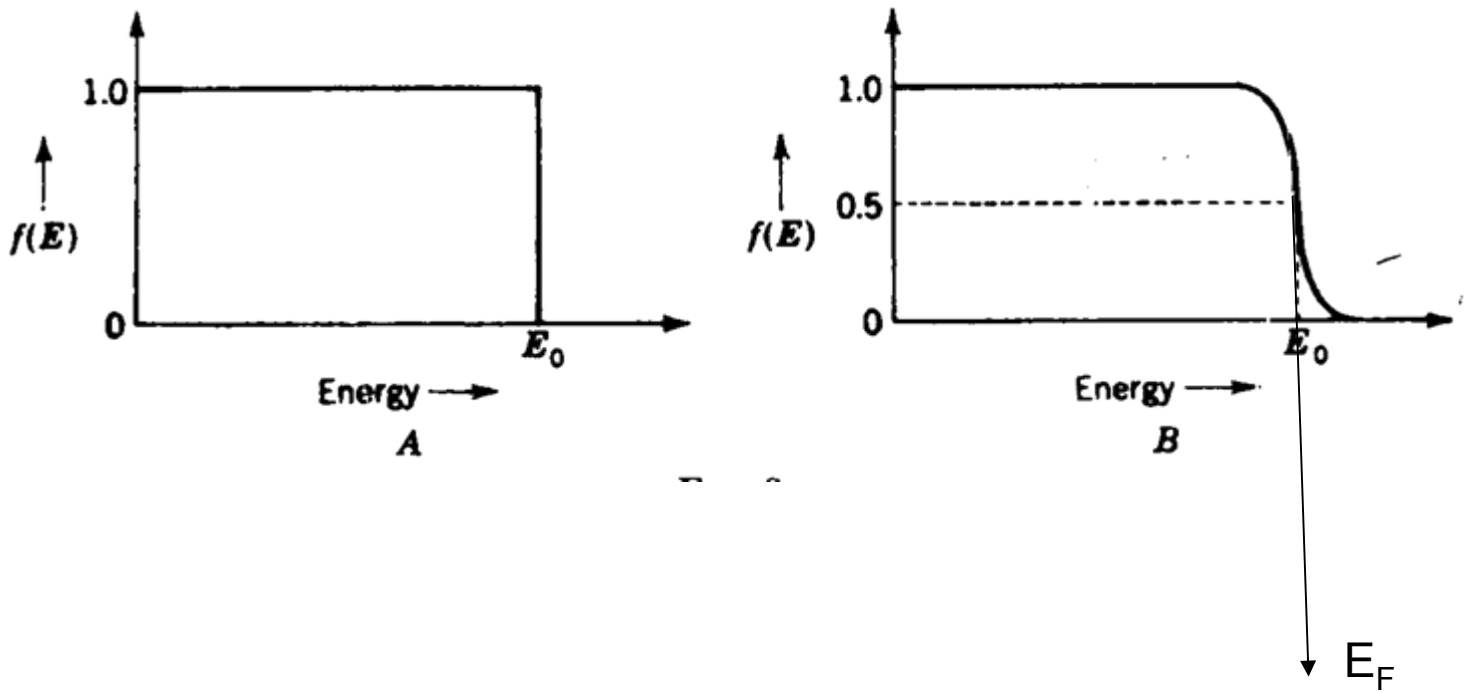

How the given energy states are occupied at a given temperature is given by Fermi-Dirac distribution.

$$N(E)dE = f(E)S(E)dE$$
$$= S(E)dE/[e^{(E-\mu)/kT} + 1]$$

N(E) = number of electrons per unit volume, having energy between E and E + dE
S(E) = number of available quantum states in this energy range.

This distribution obeys Pauli exclusion principle.
Number of electrons N(E) can never be larger than the number of available states S(E) as the denominator is always greater than one.

For states with energies well above μ, 1 in the denominator can be neglected.
$N(E)dE \approx e^{-(E-\mu)/kT}$ This resembles Bolzmann distribution

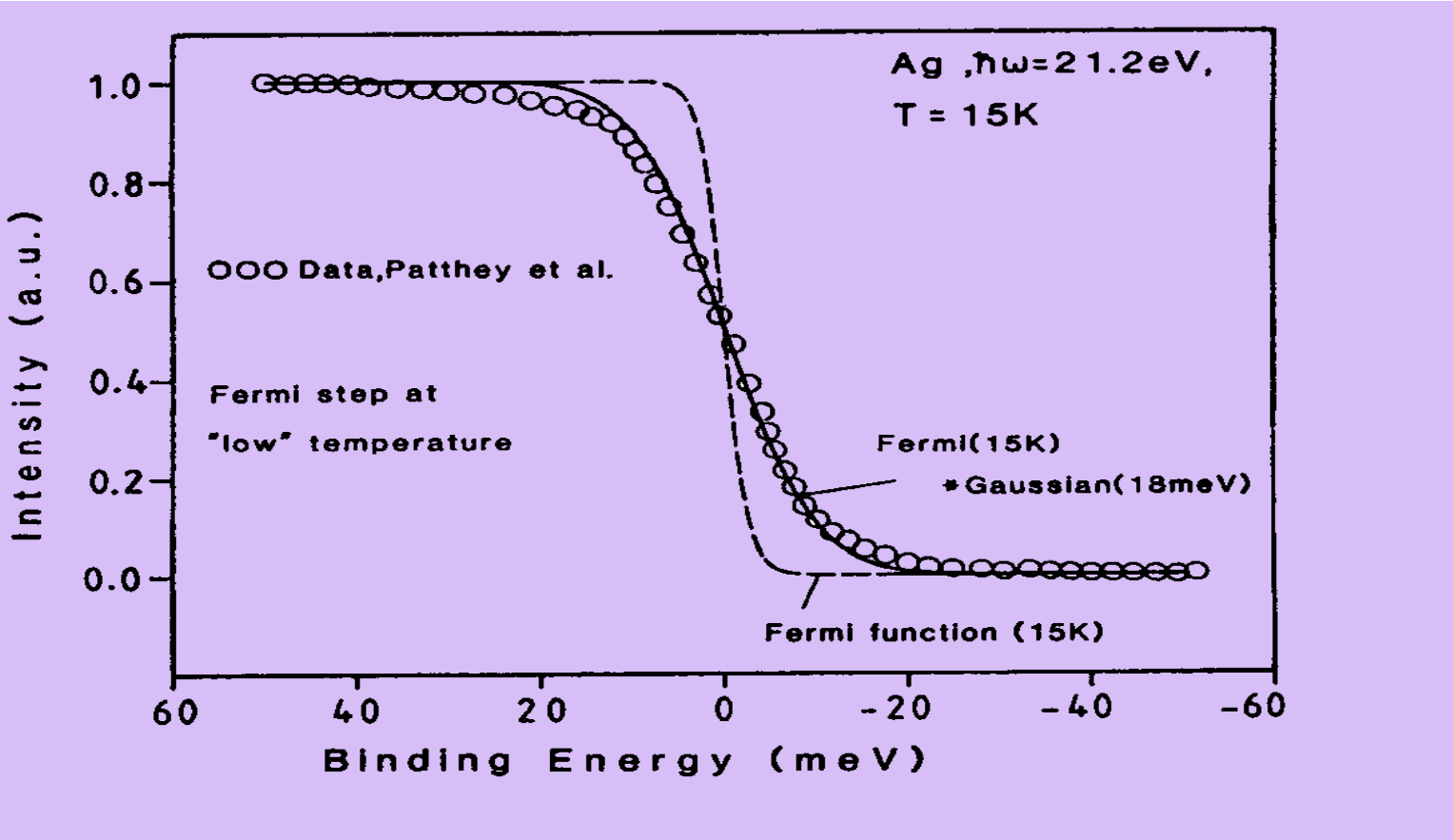


**UPS EDC at $E_F$ of Ag (15 K). Resolution, $\Delta E$ is obtained by convoluting a Fermi function with a Gaussian function**

# Analysers

# Retarding Field Analyser

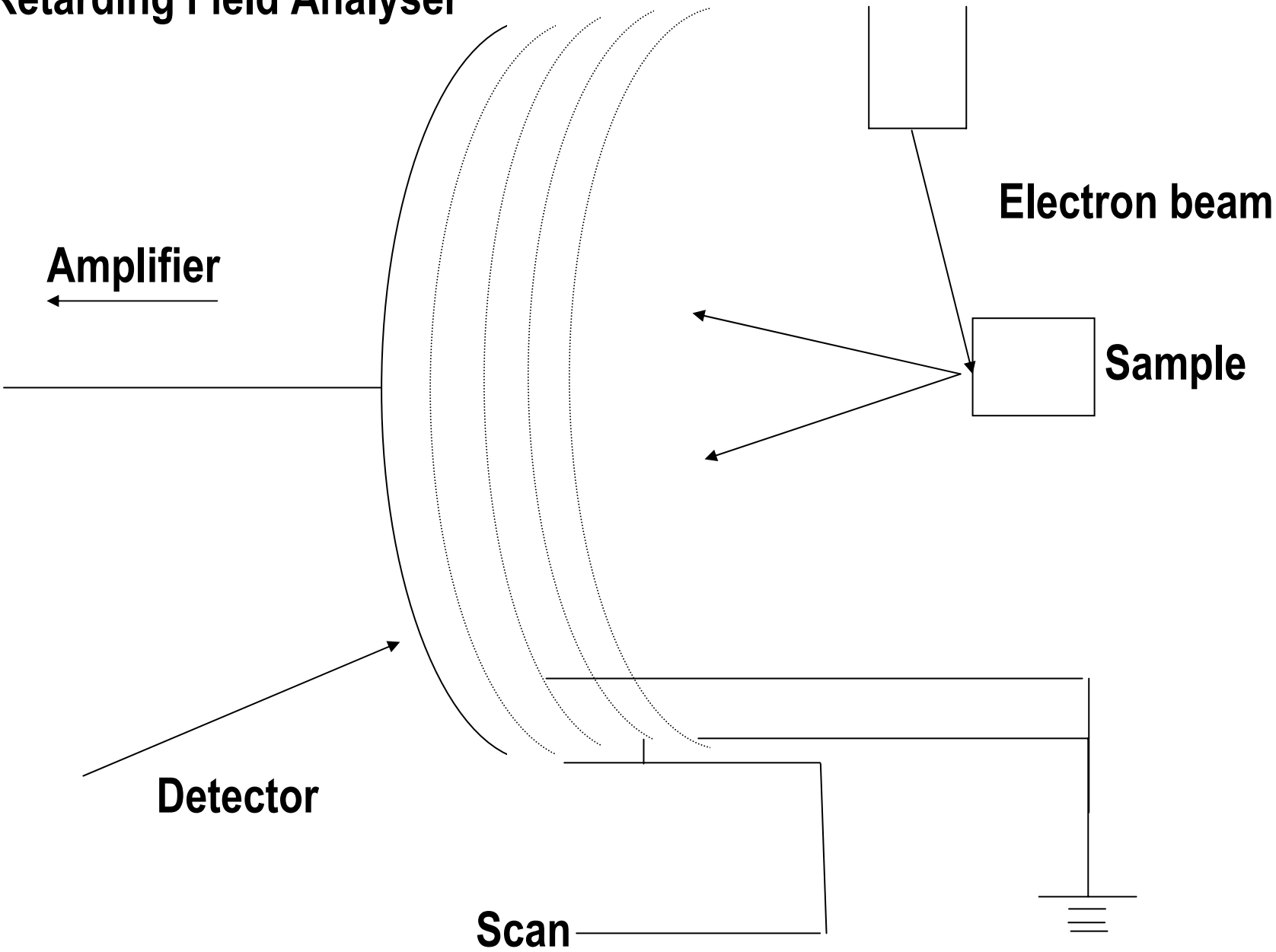

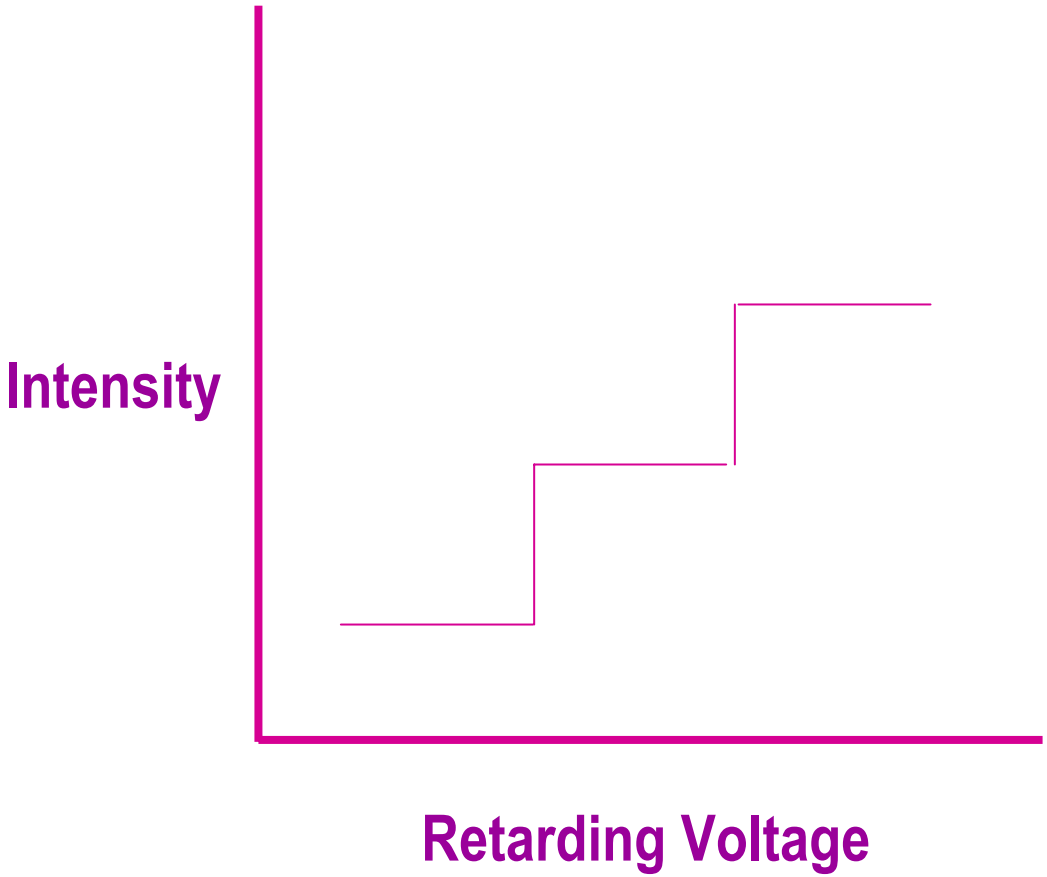
Intensity
Retarding Voltage

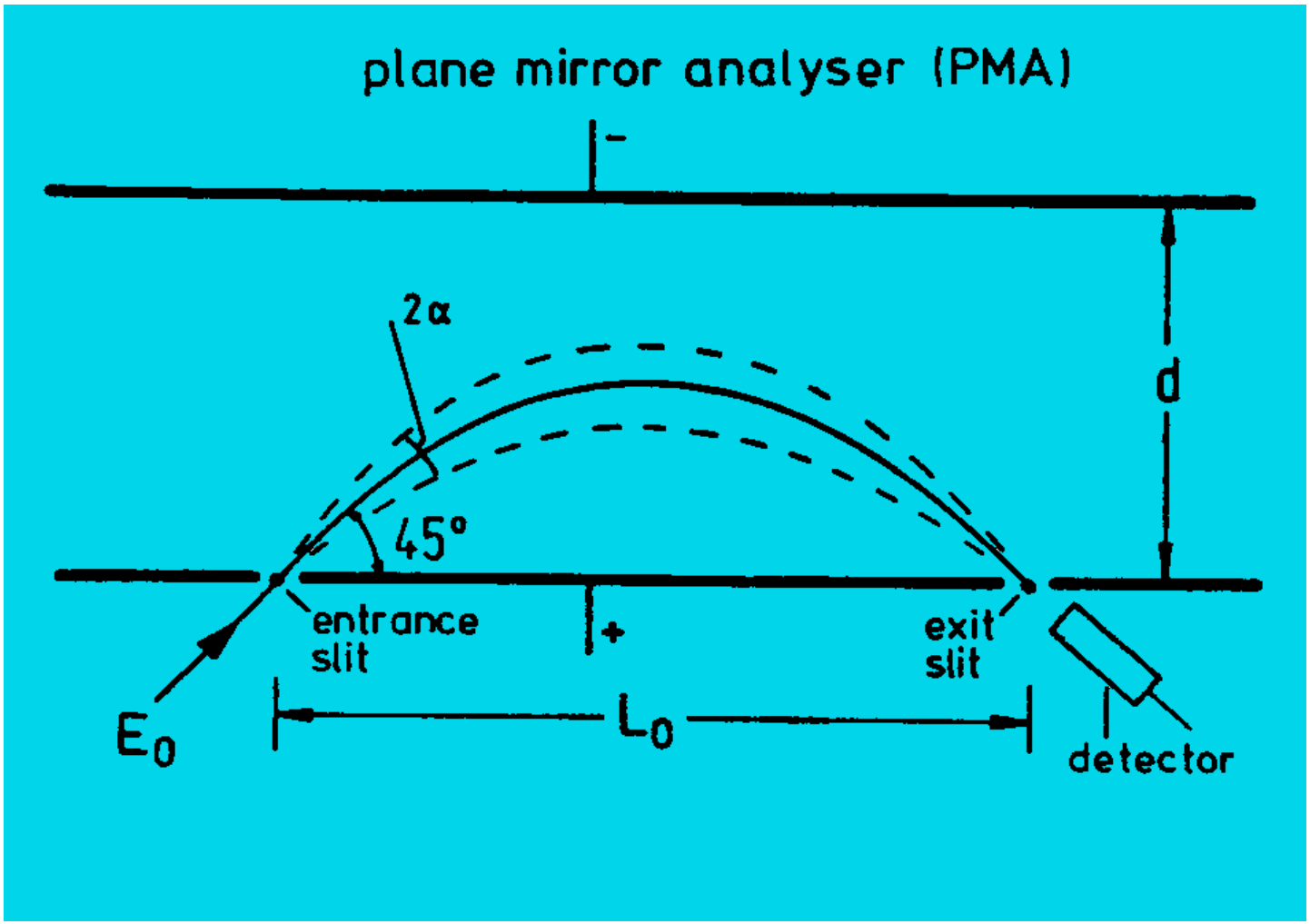
plane mirror analyser (PMA)
-
2α
d
45°
entrance
slit
+
exit
slit
E0
L0
detector

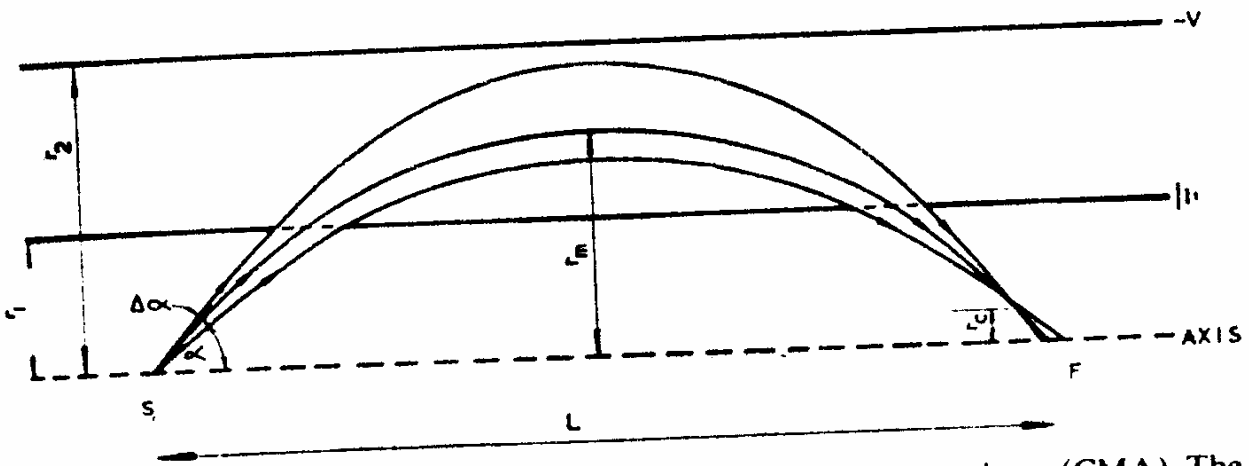


Figure 2.22 Diagrammatic arrangement of a cylindrical mirror analyser (CMA). The radii are $r_1$ for the inner cylinder and $r_2$ for the outer cylinder. The inner cylinder is earthed and a potential $-V$ is applied to the outer cylinder. Electrons emitted from a source S on the axis with a kinetic energy $E_o$ are re-focused at F according to the expression (2.10). The entrance angle $\alpha$ is chosen to be 42° 18′, since at that angle the CMA becomes a second-order focusing device. A typical angular aperture $\Delta\alpha$ would be 6°. $L$ is the distance between S and F, $r_c$ is the position of the minimum trace width and $r_m$ the maximum distance off the axis for electrons entering the analyser at 42° 18′. (After Bishop, Coad and Rivière[36])

$$E_o/eV = k/\ln(r_2/r_1) \quad mv^2/r = eV$$

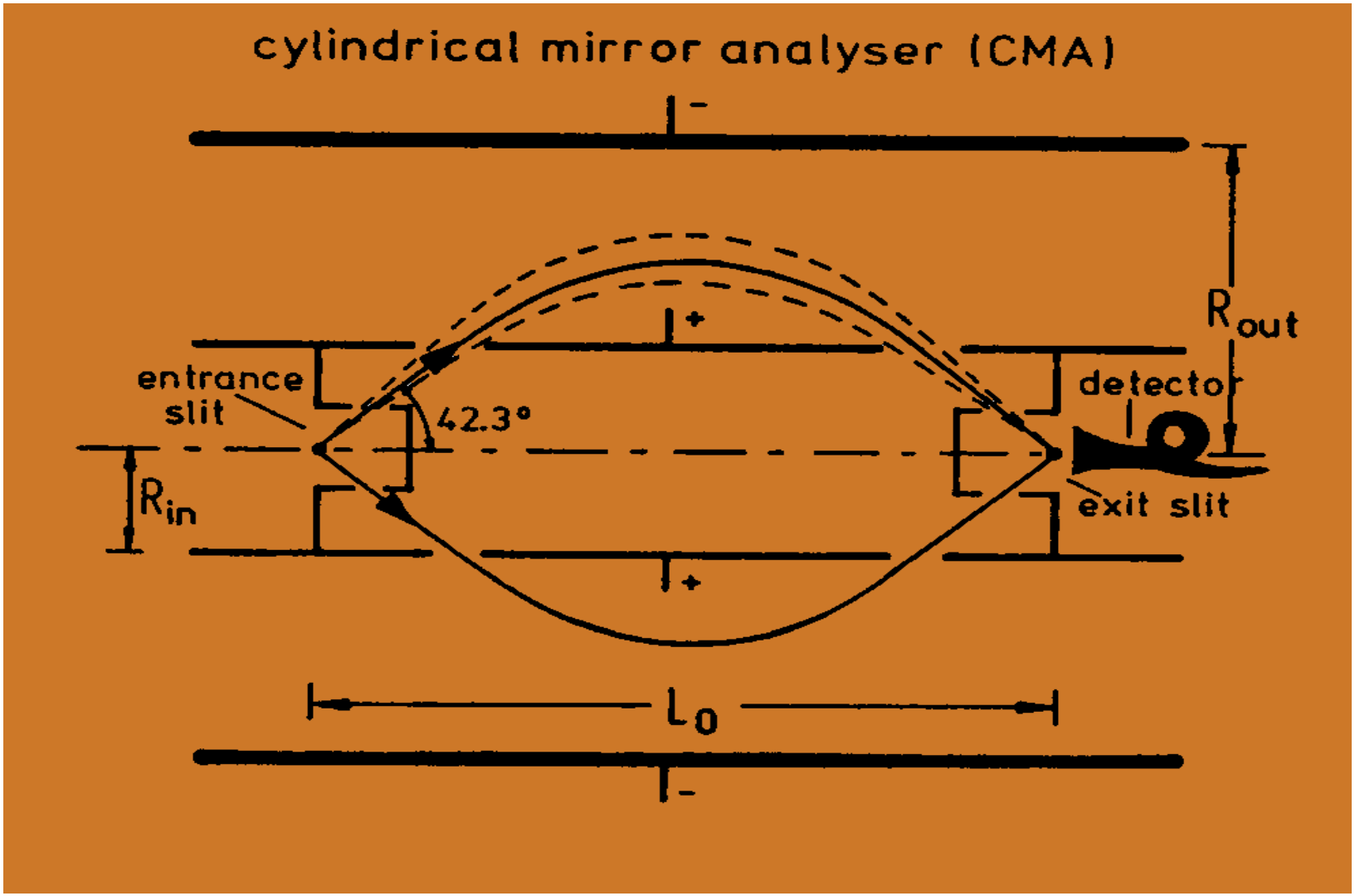
cylindrical mirror analyser (CMA)
-
+
+
-
entrance slit
42.3°
detecto
exit slit
$R_{out}$
$R_{in}$
$L_0$

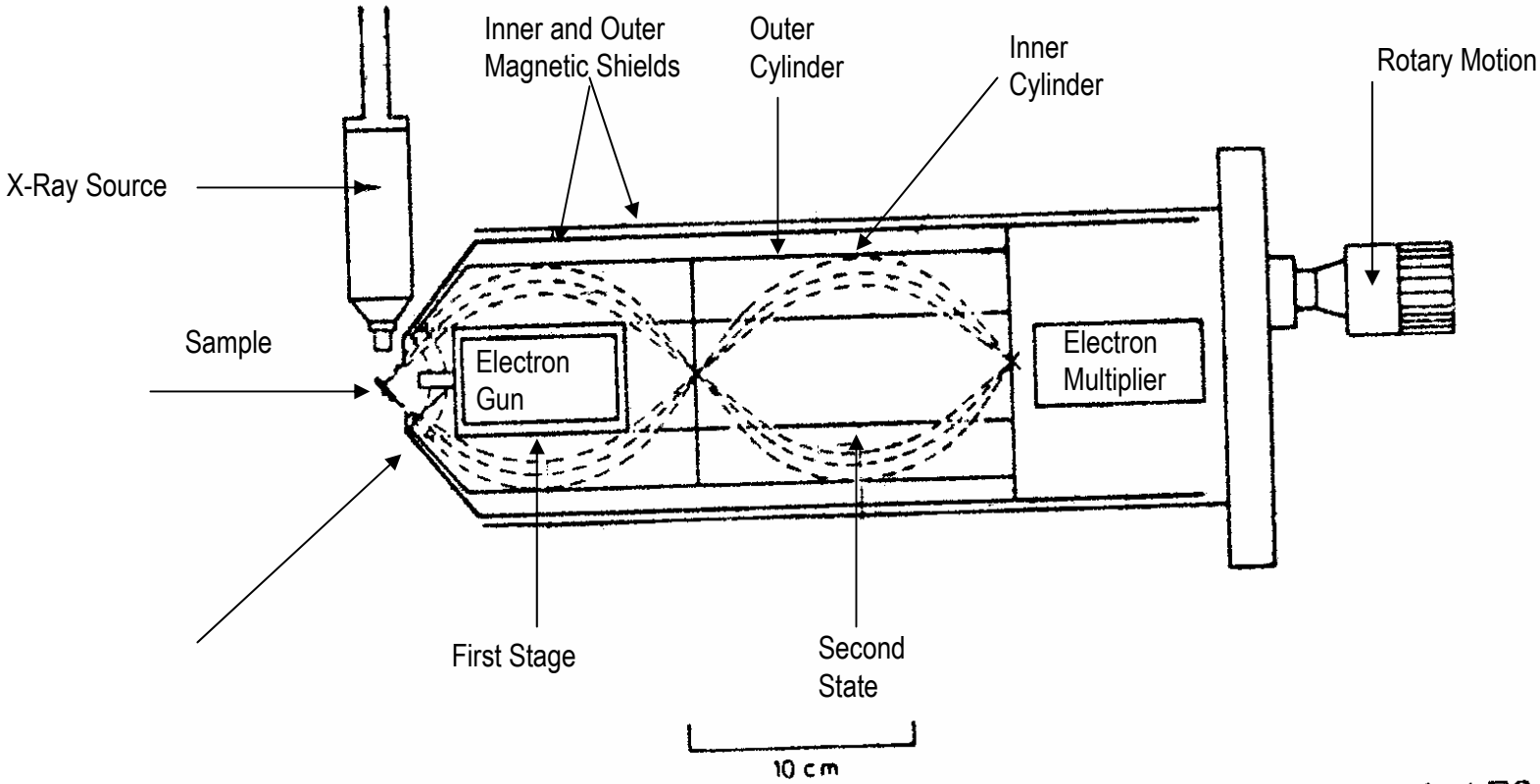


Figure 2.23 Diagrammatic arrangement of a double-pass CMA, used for both AES and XPS. The exit aperture from the first stage is the entrance aperture to the second stage. At the front end of the analyser are two spherical retarding grids centred on the source area of the sample that retard photo-electrons to a constant pass energy for XPS, For AES the grids are at earth potential, as is the inner cylinder. An externally operated rotary motion allows the entrance and exit apertures to the second stage to be changed remotely, from large sizes for XPS to small sizes for AES. The electron gun is situated on the axis of the CMA internally, but the X-ray source, of the type seen in detail in Figure 2.9(a), is external and positioned as close to the sample as the geometry will allow. (Reproduced from Palmberg[40] by permission of Elsevier Scientific Publishing Company)

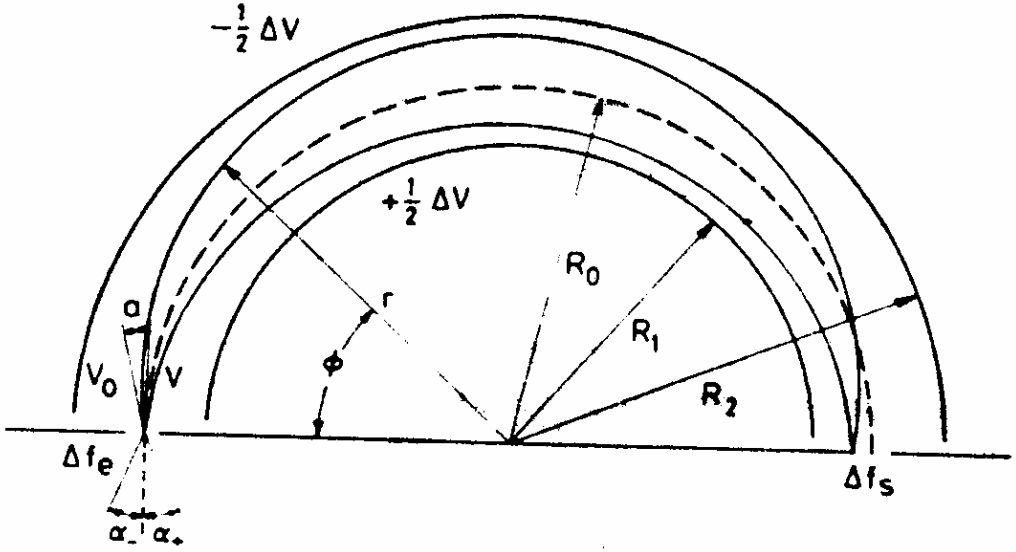


Figure 2.24 Principle of operation of the concentric hemispherical analyser. Two hemispherical surfaces of inner radius $R_1$ and outer radius $R_2$ are positioned concentrically. A potential $\Delta V$ is applied between the surfaces so that the outer is negative and the inner positive with respect to $\Delta V$. $R_0$ is the median equipotential surface between the hemispheres, and the entrance and exit slits are both centred on $R_0$. If $E$ is the kinetic energy of an electron travelling in an orbit of radius $R_0$, then the relationship between $E$ and $V$ is given by expression (2.21). $\phi$ and $r$ are the angular and radial coordinates, respectively, of an electron of energy $E_0$ ($= e\Delta V_0$) entering the analyser at an angle $\alpha$ to the slit normal. If this electron is to pass through the exit slit, its path in the analyser is governed by the conditions of expression (2.22). (Reproduced from Roy and Carette[43] by permission of the National Research Council of Canada)

$$e\Delta V = E(R_2/R_1 - R_1/R_2)$$

# cylindrical deflection analyser (CDA)

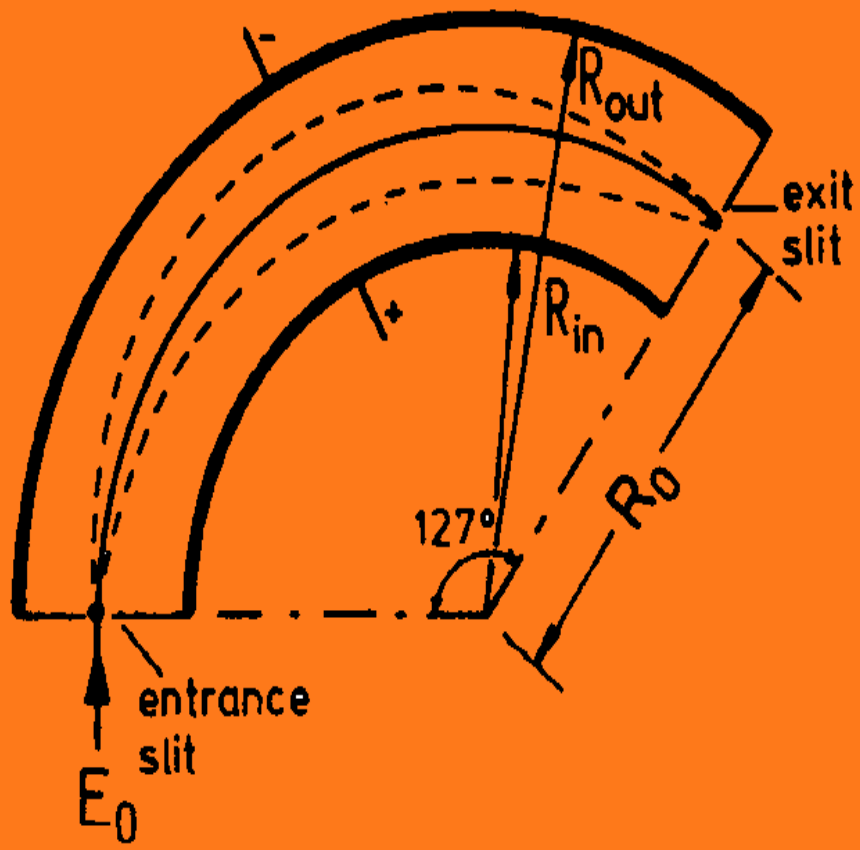

# spherical deflection analyser (SDA)

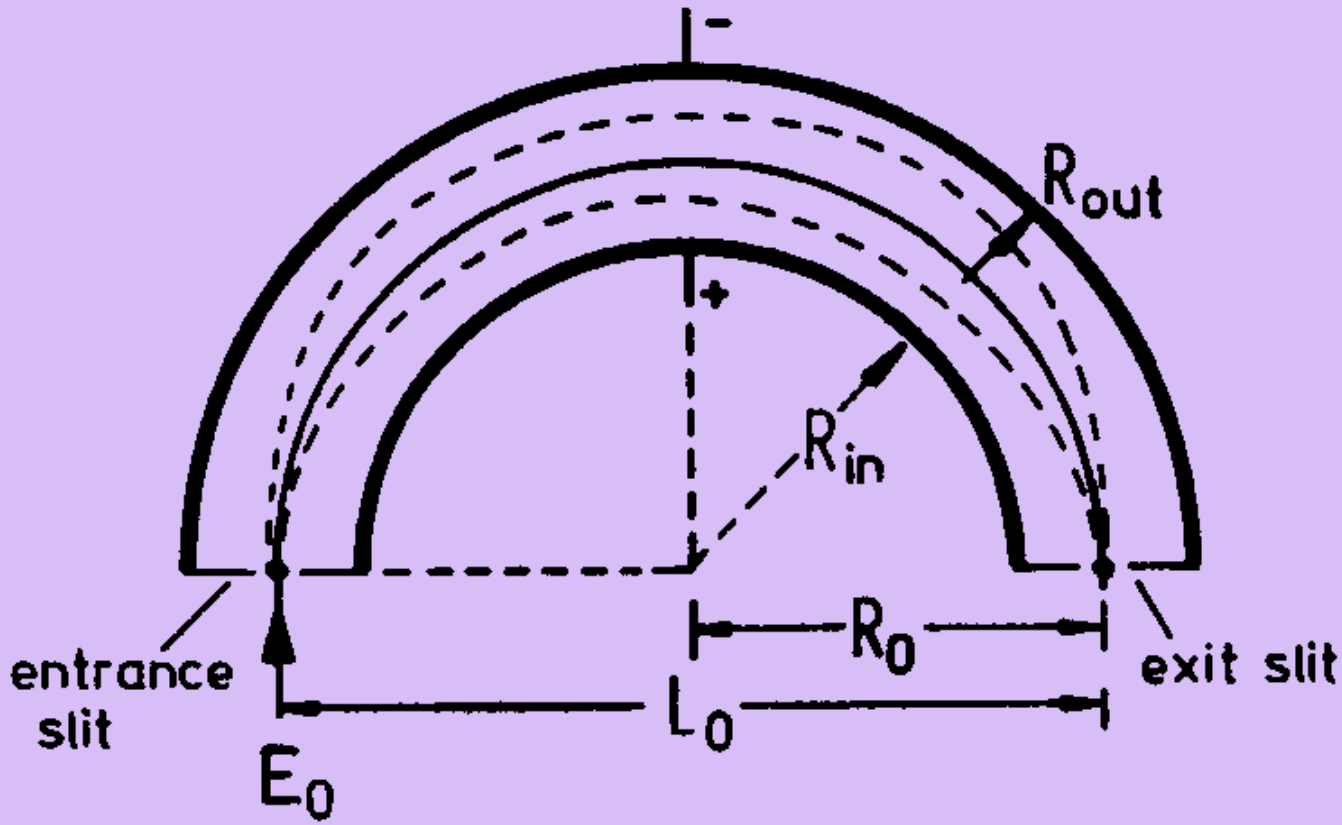

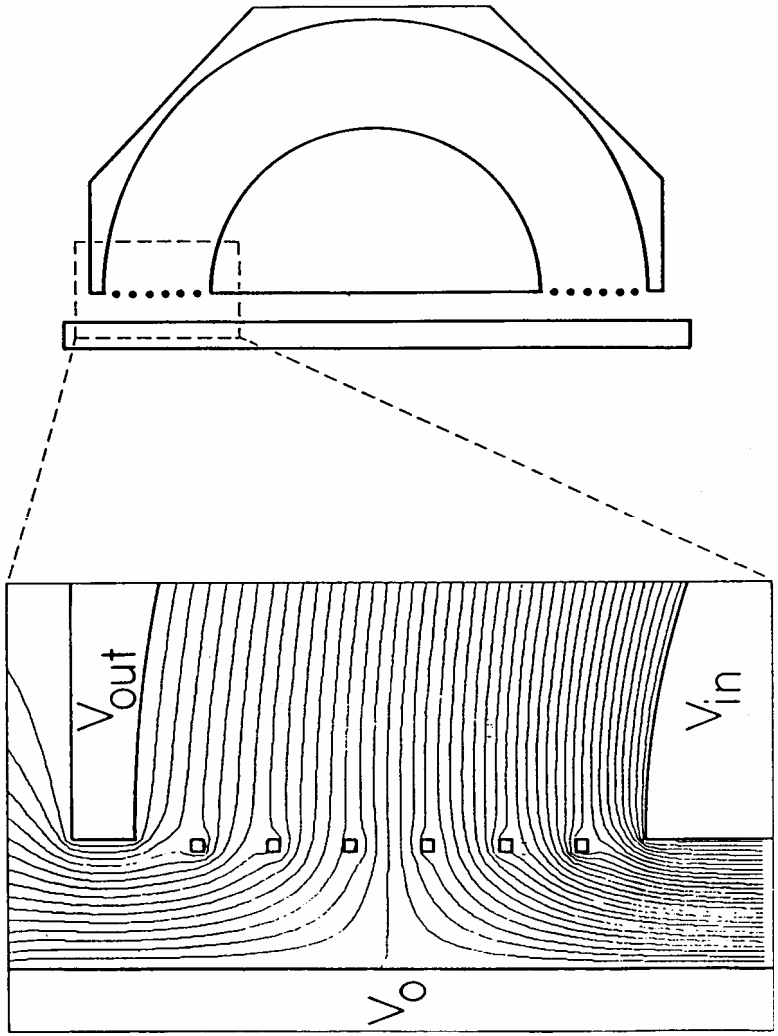
$V_{out}$
$V_{in}$
$V_0$

# 1. Single-Channel Detector

**Channel electron multiplier:A continuous dynode surface. High count rate of $10^6$ counts per second.**

# 2. Multi-Channel Detector

**A set of parallel detector chains or position sensitive detectors kept at the analyser exit slit plain.**

# Channel electron multiplier

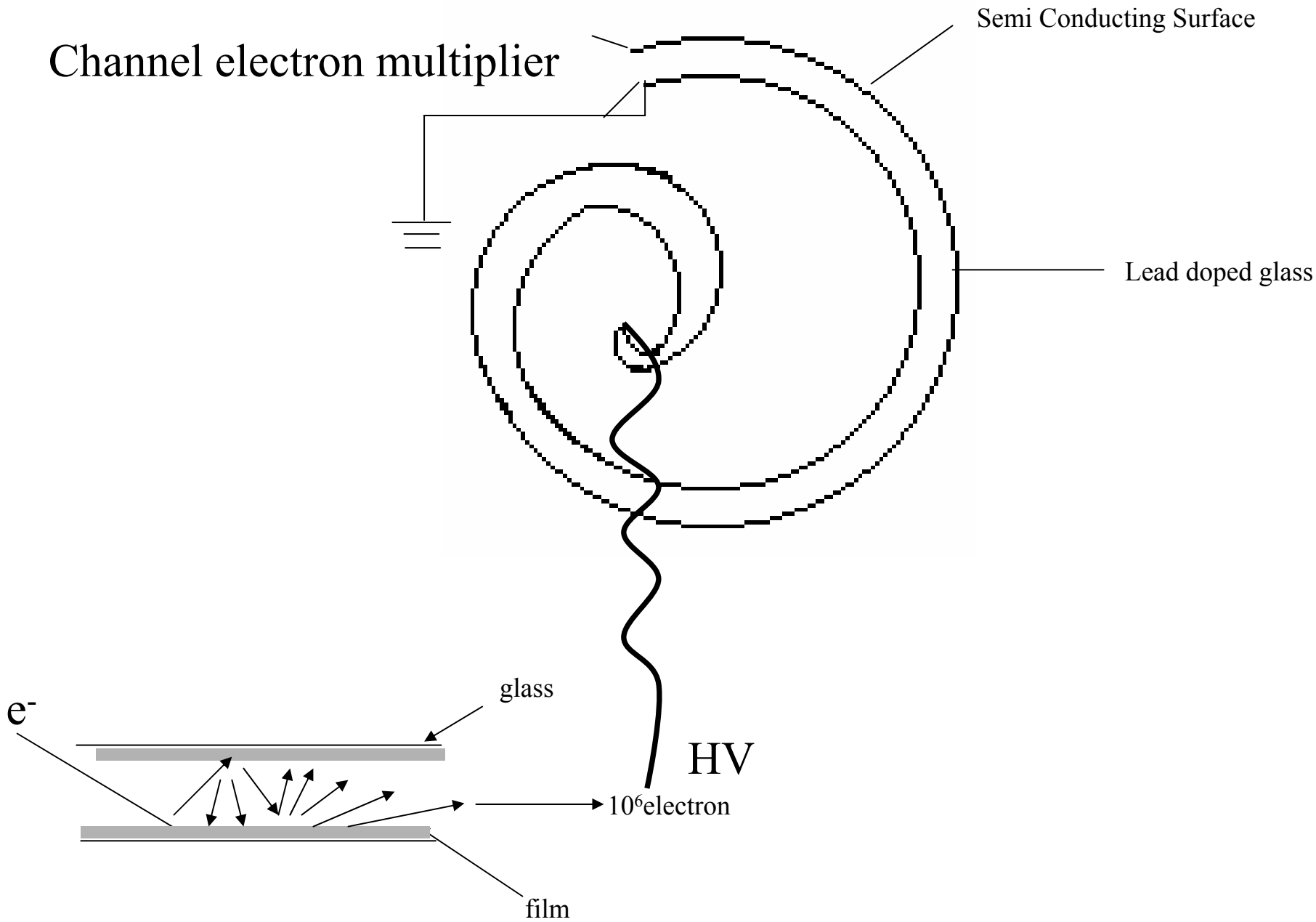

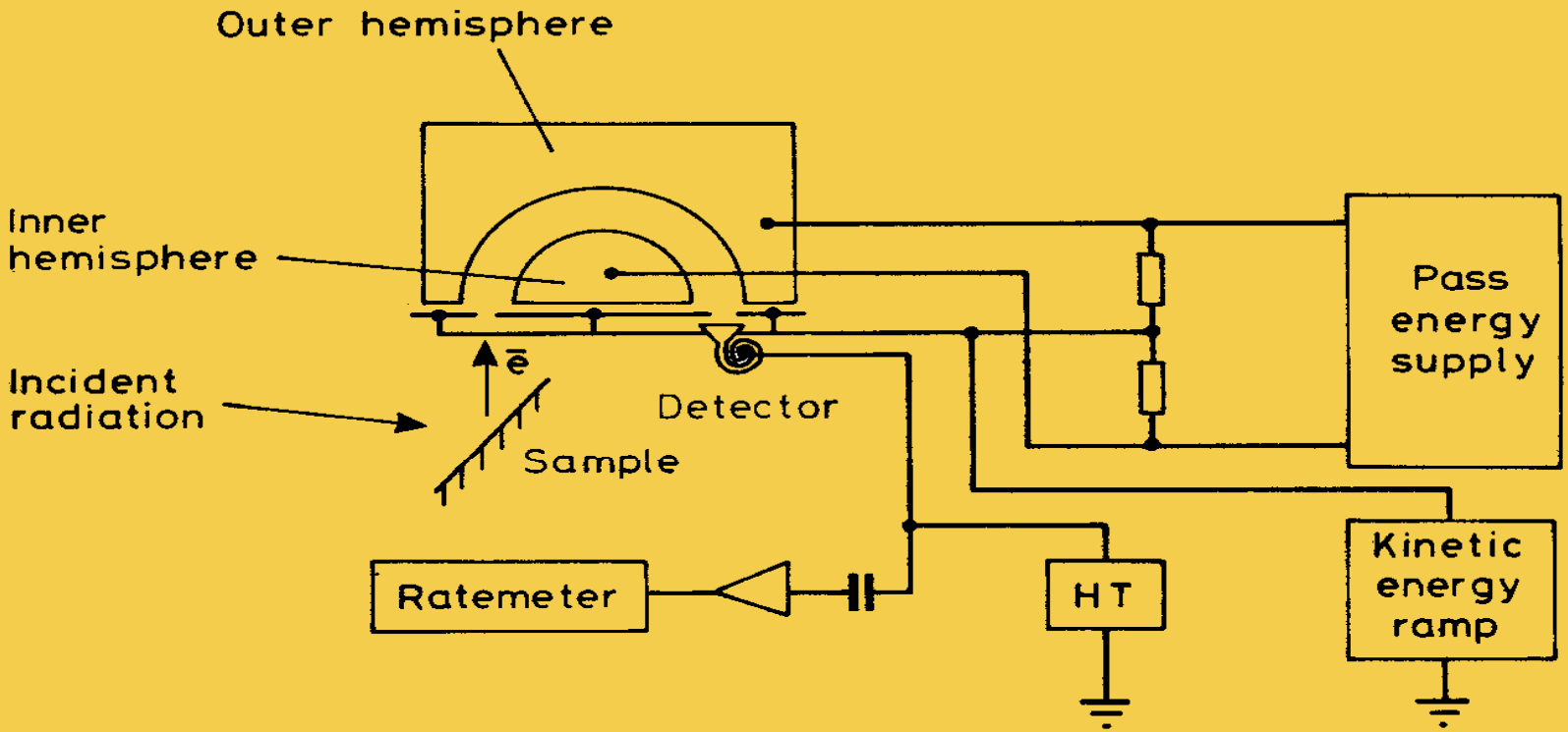


# Hemispherical sector electron energy analyser and control electronics.

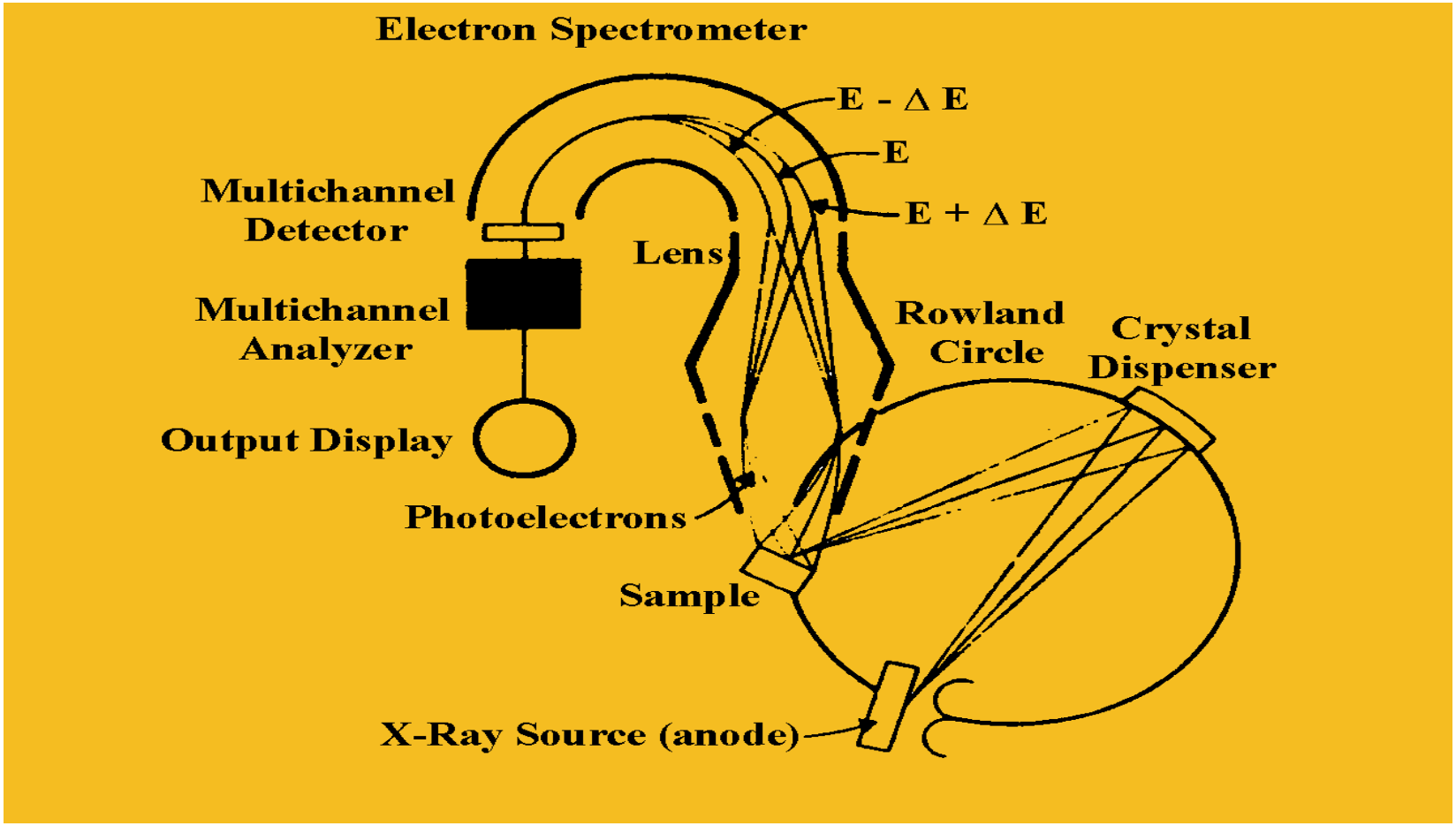


# Spectrometer with X-ray monocromatisation

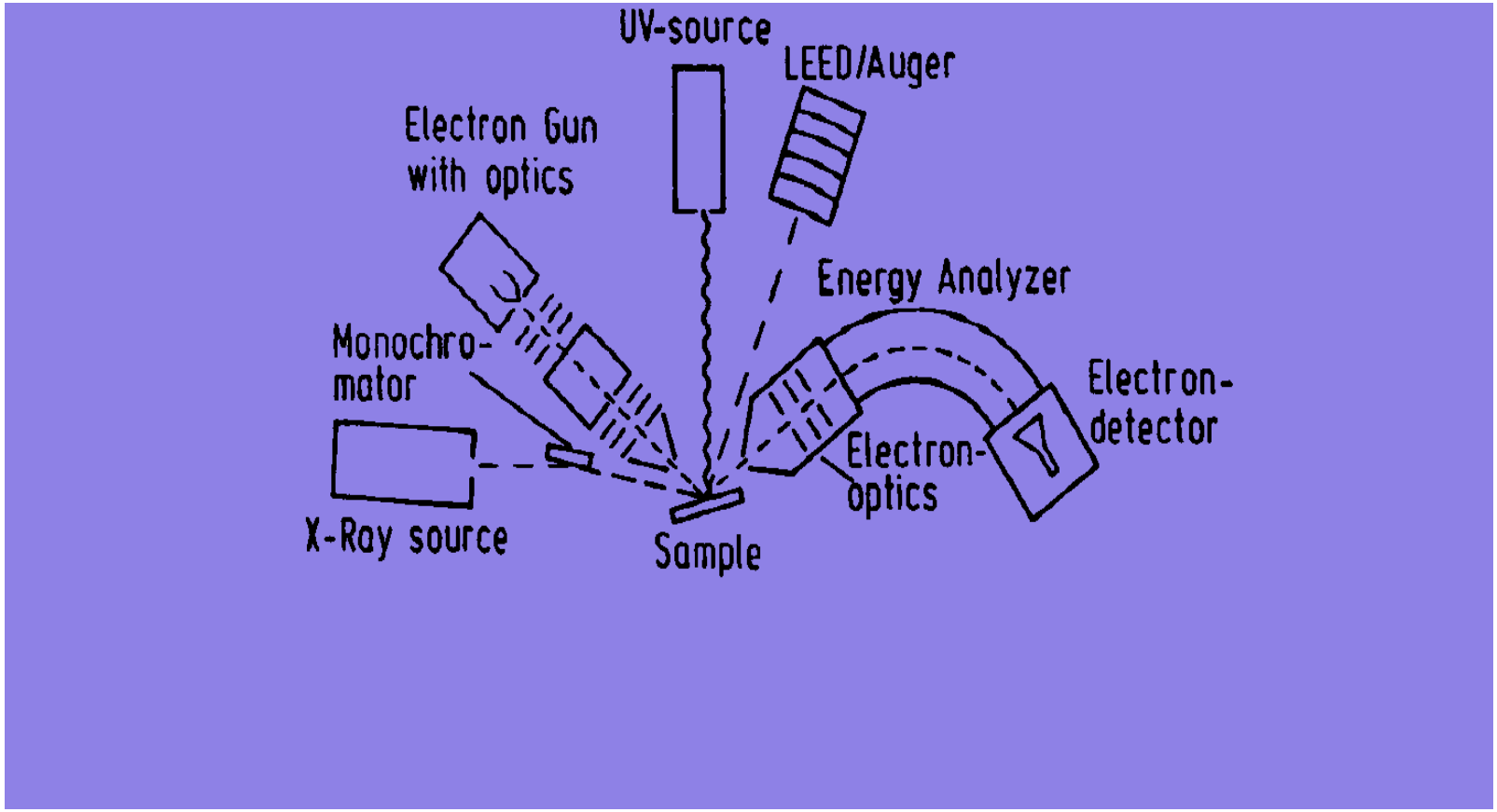


# Modern instrument for UPS, XPS, AES and EELS

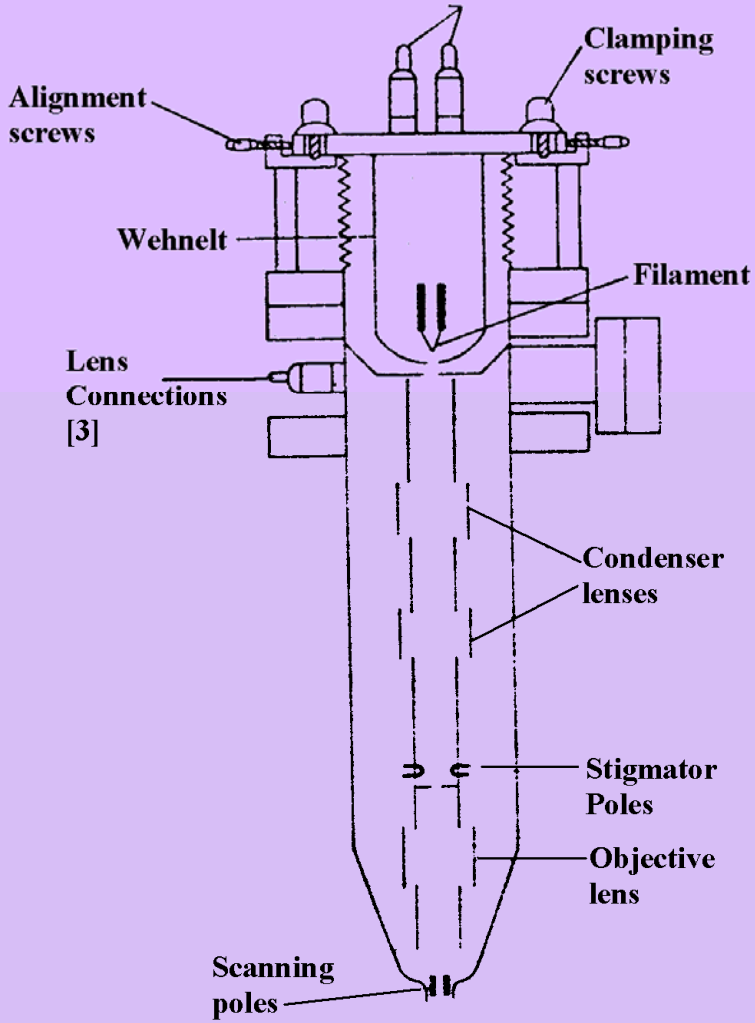


# An electron gun for beams up to 10 ke V

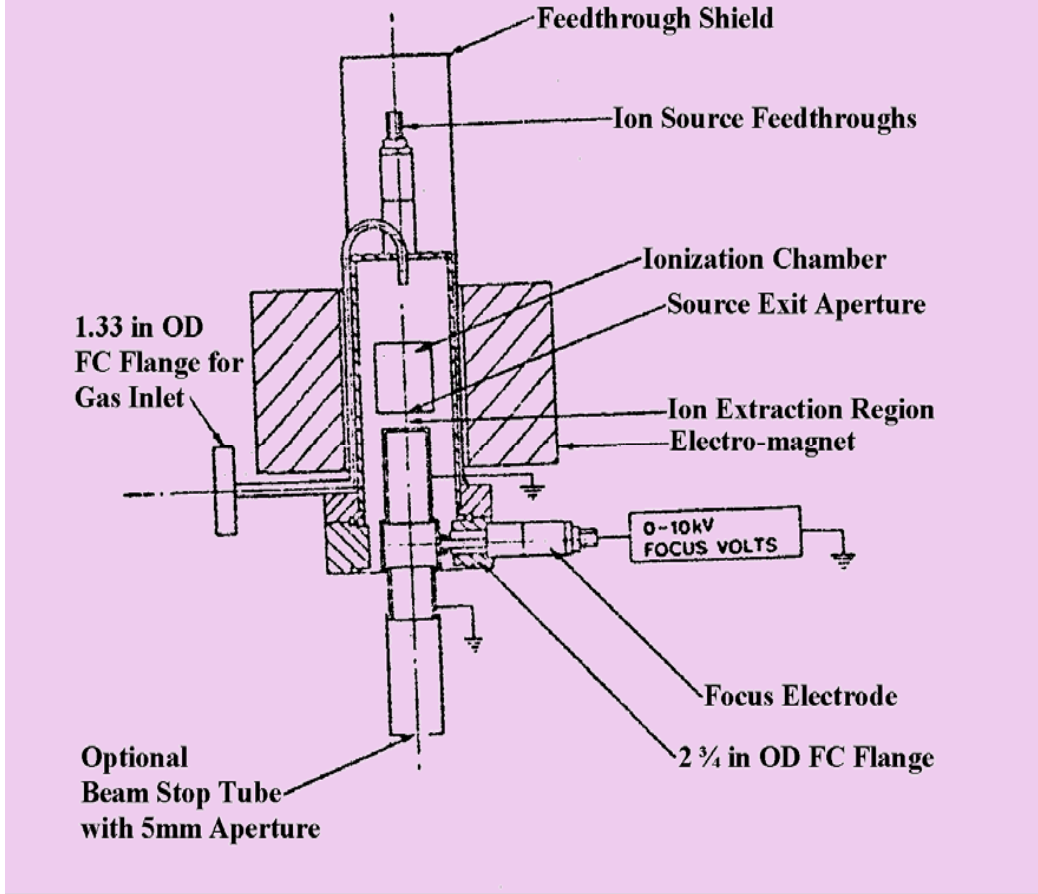


# Ion gun using a Penning discharge.

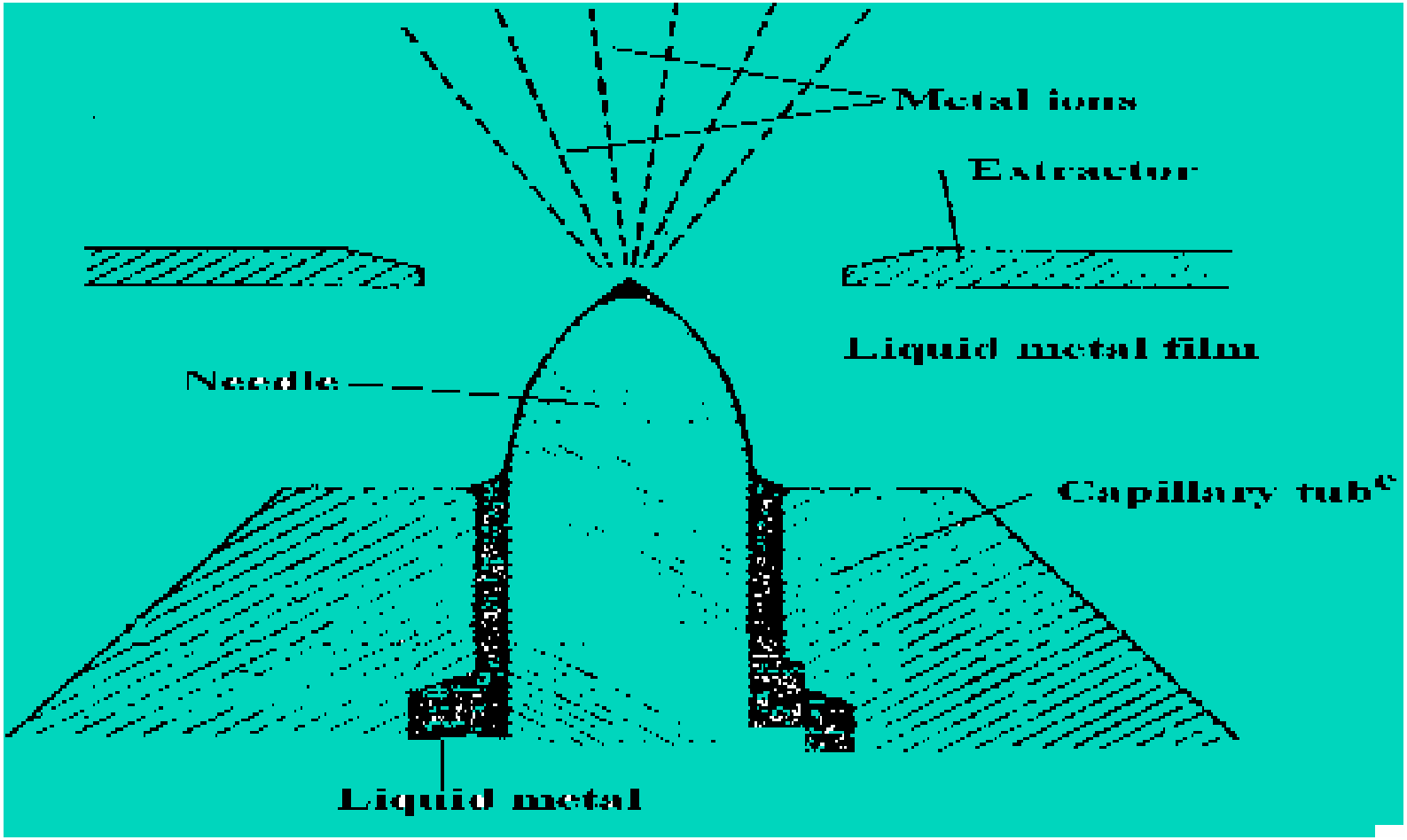


# A liquid-metal field emission ion source

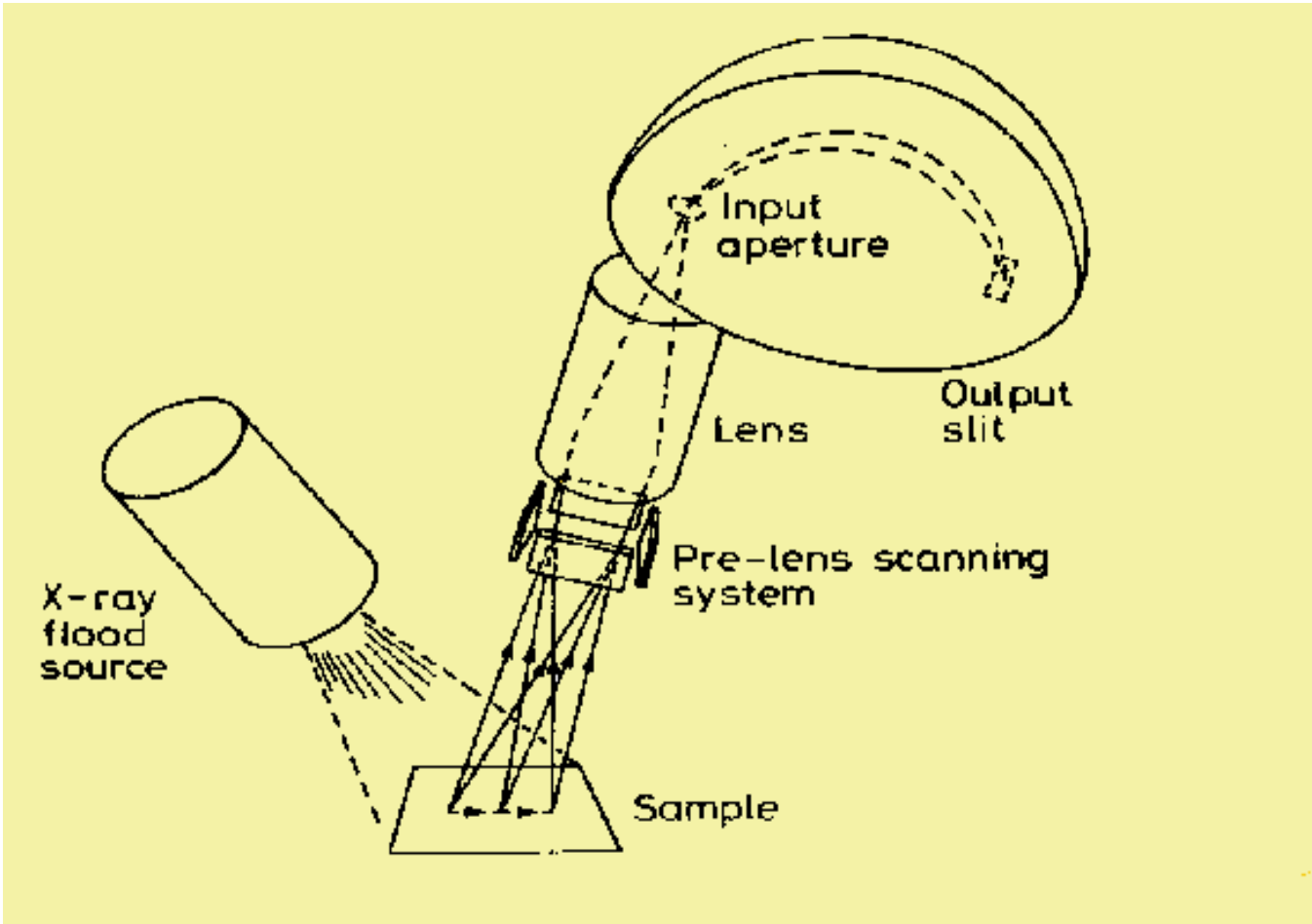


# A simple method of XPS imaging using a conventional HAS instrument

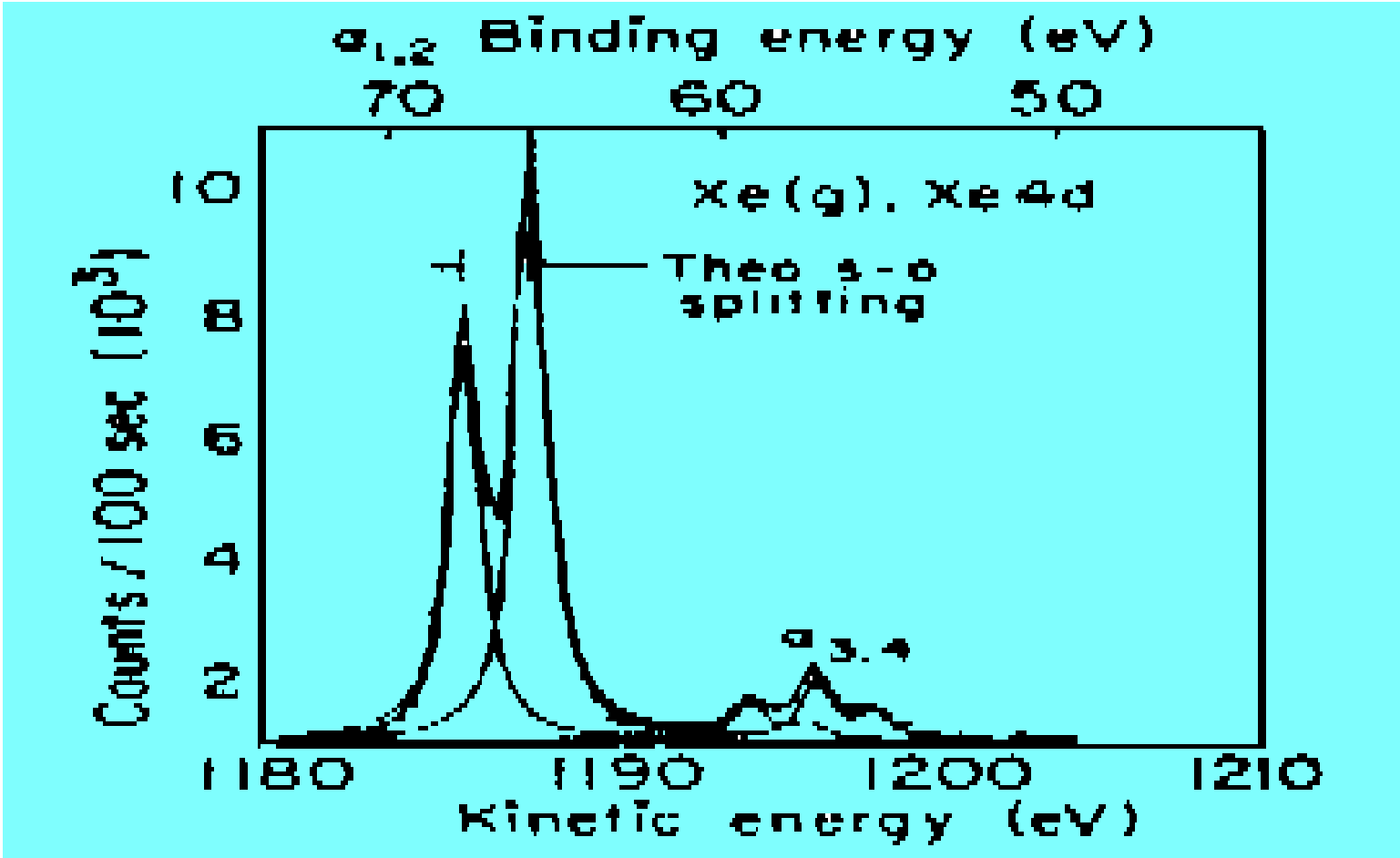


Data analysis